CARDIFF UNIVERSITY
PRIFYSGOL CAERDYDD

ORCA – Online Research @ Cardiff

This is an Open Access document downloaded from ORCA, Cardiff University's institutional repository:https://orca.cardiff.ac.uk/id/eprint/60878/

This is the author's version of a work that was submitted to / accepted for publication.

Citation for final published version:

Kakar, Mohammad Ishaq, Kerr, Andrew Craig , Mahmood, Khalid, Collins, Alan S., Khan, Mehrab and McDonald, Iain 2014. Supra-subduction zone tectonic setting of the Muslim Bagh Ophiolite, northwestern Pakistan: Insights from geochemistry and petrology. Lithos 202-20 , pp. 190-206. 10.1016/j.lithos.2014.05.029

Publishers page: http://dx.doi.org/10.1016/j.lithos.2014.05.029

Please note:
Changes made as a result of publishing processes such as copy-editing, formatting and page numbers may not be reflected in this version. For the definitive version of this publication, please refer to the published source. You are advised to consult the publisher's version if you wish to cite this paper.

This version is being made available in accordance with publisher policies. See http://orca.cf.ac.uk/policies.html for usage policies. Copyright and moral rights for publications made available in ORCA are retained by the copyright holders.

Accepted Manuscript

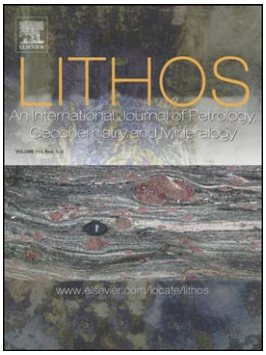

Supra-subduction zone tectonic setting of the Muslim Bagh Ophiolite, northwestern Pakistan: Insights from geochemistry and petrology

Mohammad Ishaq Kakar, Andrew C. Kerr, Khalid Mahmood, Alan S. Collins, Mehrab Khan, Iain McDonald

PII: S0024-4937(14)00193-5
DOI: doi: 10.1016/j.lithos.2014.05.029
Reference: LITHOS 3302

To appear in: *LITHOS*

Received date: 30 October 2013
Revised date: 31 May 2014
Accepted date: 31 May 2014

Please cite this article as: Kakar, Mohammad Ishaq, Kerr, Andrew C., Mahmood, Khalid, Collins, Alan S., Khan, Mehrab, McDonald, Iain, Supra-subduction zone tectonic setting of the Muslim Bagh Ophiolite, northwestern Pakistan: Insights from geochemistry and petrology, *LITHOS* (2014), doi: 10.1016/j.lithos.2014.05.029

This is a PDF file of an unedited manuscript that has been accepted for publication. As a service to our customers we are providing this early version of the manuscript. The manuscript will undergo copyediting, typesetting, and review of the resulting proof before it is published in its final form. Please note that during the production process errors may be discovered which could affect the content, and all legal disclaimers that apply to the journal pertain.

ACCEPTED MANUSCRIPT

Supra-subduction zone tectonic setting of the Muslim Bagh Ophiolite, northwestern Pakistan: insights from geochemistry and petrology.

Mohammad Ishaq Kakar[1], Andrew C. Kerr[2]*, Khalid Mahmood[3], Alan S. Collins[4], Mehrab Khan[5], Iain McDonald[2]

[1]*Centre of Excellence in Mineralogy, University of Balochistan, Quetta, Pakistan.*

[2]*School of Earth and Ocean Sciences, Cardiff University, Main Building, Park Place, Cardiff, Wales, CF10 3AT, UK.*

[3]*Department of Earth Sciences, University of Sargodha, Sargodha, Pakistan.*

[4]*Tectonics, Resources and Exploration (TRaX), School of Earth and Environmental Sciences, University of Adelaide, SA 5005, Australia.*

[5]*Department of Geology, University of Balochistan, Quetta, Pakistan.*

* Corresponding author. *E-mail address: kerra@cf.ac.uk (A.C. Kerr).*

ACCEPTED MANUSCRIPT

Abstract

The geology of the Muslim Bagh area comprises the Indian passive continental margin and suture zone, which is overlain by the Muslim Bagh Ophiolite, Bagh Complex and a Flysch Zone of marine–fluvial successions. The Muslim Bagh Ophiolite has a nearly-complete ophiolite stratigraphy. The mantle sequence of foliated peridotite is mainly harzburgite with minor dunite and contains podiform chromite deposits that grade upwards into transition zone dunite. The mantle rocks (harzburgite/dunite) resulted from large degrees of partial melting of lherzolite and have also been affected by melt–

ACCEPTED MANUSCRIPT

peridotite reaction. The Muslim Bagh crustal section has a cyclic succession of ultramafic-mafic cumulate with dunite at base, that grades into wehrlite/pyroxenite with gabbros (olivine gabbro, norite and hornblende gabbro) at the top. The sheeted dykes are immature in nature and are rooted in crustal gabbros. The dykes are mainly metamorphosed dolerites, with minor intrusions of plagiogranites. The configuration of the crustal section indicates that the crustal rocks were formed over variable time periods, in pulses, by a low magma supply rate. The whole rock geochemistry of the gabbros, sheeted dykes and the mafic dyke swarm suggests that they formed in a supra-subduction zone tectonic setting in Neo-Tethys during the Late Cretaceous. The dykes of the mafic swarm crosscut both the ophiolite and the metamorphic sole rocks and have a less-marked subduction signature than the other mafic rocks. These dykes were possibly emplaced off-axis and can be interpreted to have been generated in the spinel peridotite stability zone i.e., <50-60km, and to have risen through a slab window. The Bagh Complex is an assemblage of Triassic–Cretaceous igneous and sedimentary rocks, containing tholeiitic, N-MORB-like basalts and alkali basalts with OIB-type signatures. Nb-Ta depletion in both basalt types suggests possible contamination from continental fragments incorporated into the opening Tethyan oceanic basin during break-up of Gondwana. The lithologies and ages of the Bagh Complex imply that these rocks formed in an area extending from the continental margin over the Neo-Tethyan ocean floor. The Bagh Complex was then juxtaposed with the Muslim Bagh Ophiolite in the final stage of tectonic emplacement.

Keywords: ophiolite; Tethyan; Bagh Complex; geochemistry; Cretaceous

ACCEPTED MANUSCRIPT

1. Introduction

Ophiolites are fragments of oceanic lithosphere that have been emplaced tectonically along continental margins in accretionary prisms during orogenic processes. They are either intact; having almost a complete stratigraphy, or are preserved in a dismembered state i.e., an ophiolitic mélange (e.g., Robertson, 2002). The Muslim Bagh Ophiolite, in Balochistan, Pakistan is a relatively intact ophiolite consisting of thick mantle peridotites, with a mantle-crust transition zone which passes into layered ultramafic–mafic cumulates and a less well-developed sheeted dyke complex with no basaltic extrusive cover (Figures 1; 2).

Two tectonic models have been proposed for Muslim Bagh Ophiolite; a) a back-arc basin (BAB) setting (Siddiqui et al., 1996) and a composite tectonic setting (Khan et al., 2007). The latter has divided the ophiolite into two nappes; 1) an ophiolite sequence of island arc affinity and 2) the underlying Bagh Complex which was interpreted to have formed in a mid-ocean ridge setting. However, detailed mapping of the ophiolite (Kakar, 2011), the Bagh Complex (Mengal et al., 1994; Naka et al., 1996) and the metamorphic sole (Kakar et al., 2012) along with the new geochemical analysis reported in this paper, indicates that both previous interpretations are problematic. The objectives of this paper are therefore to test and evaluate the previous hypotheses about the origin and mechanism of emplacement of the ophiolite using new detailed petrological and geochemical data.

2. Regional tectonic setting and geology of the Muslim Bagh area

The rocks of the Muslim Bagh area along with the Bela, Khanozai, Zhob and Waziristan ophiolites originally formed part of the Neo-Tethyan Ocean and are exposed along the western suture zone between the Asian and Indian plates (e.g., Asrarullah et al., 1979; Sengor, 1987).

ACCEPTED MANUSCRIPT

During the late Jurassic and early Cretaceous, India separated from Western Australia (Powell et al., 1988; Muller et al., 2000) and Antarctica (Ali and Aitchison, 2005) (Figure 3a).

The Bagh Complex consists of two main volcanic units: a) oceanic tholeiite to alkaline basalts intercalated with pelagic sediments and known as the basalt-chert unit (Bbc), and b) a basaltic hyaloclastite-mudstone unit (Bhm). The ages of these volcanic units range from Early-Late Cretaceous and Albian-Maastrichtian, respectively (Kojima et al., 1994). A very similar basalt-chert unit is also reported below the Waziristan Ophiolite (Beck et al., 1995, 1996), the Bela Ophiolite (Gnos et al., 1997), and along the Indus –Yarlung Tsangbo – suture at the north of the Himalayas (Gopel et al., 1984; Xiao, 1984, Xiao et al., 2003; Malpas et al., 2003). This basalt-chert unit has been interpreted to represent the oceanic crust of Neo-Tethys, which formed during the Middle to Late Cretaceous (Figure 3b) (Kojima et al., 1994). According to Gnos et al. (1997), in the Cretaceous quiet period, reorganization of plates took place in some parts of Neo-Tethys. Part of this reorganization involved the separation of the Indian plate from Madagascar resulting in compression and subduction along the NW edge of Indian plate. The consequent arc with basic volcanism ultimately formed the present day Muslim Bagh Ophiolite.

Zircon in a plagiogranite from the Muslim Bagh Ophiolite has yielded a U-Pb crystallization age of 80.2 ± 1.5 Ma (Kakar et al., 2012) and this age is interpreted as the age of the formation of ophiolite. This age is in good agreement with K-Ar hornblende ages (81-80 Ma; Sawada et al., 1995) but in conflict with amphibole Ar-Ar ages (70.7 ±5 Ma; Mahmood et al., 1995). Hornblende has also been dated from the amphibolites in the subophiolitic metamorphic rocks and these yielded a K-Ar age of 80.5 ± 5.3 (Sawada et al., 1995) and an Ar-Ar plateau age of 68.7 ± 1.5 Ma (Mahmood et al., 1995). These younger ages have been interpreted as the age of ophiolite emplacement and if these ages are correct then the Muslim Bagh Ophiolite was

ACCEPTED MANUSCRIPT

relatively young at the time of emplacement onto the western margin of the Indian plate (Plummer, 1996; Gnos et al., 1997, Figure 3c).

Gnos et al. (1997) proposed that the final emplacement of ophiolite and the underlying Bagh Complex onto the margin of the Indian plate was coeval with the separation of India from the Seychelles micro-continent at the Cretaceous/Tertiary boundary. This emplacement also coincided with the Reunion hotspot-related volcanism of: the Deccan flood basalts (e.g., Hofmann et al., 2000; Hooper et al., 2010); basalts on the Seychelles (Plummer and Belle, 1995); volcanism along the western suture in Bela area (Gnos et al., 1998), and in the Muslim Bagh area (Mahoney et al., 2002; Kerr et al., 2010). Finally, India collided with Eurasia; in the Late Paleocene to Early Eocene period (Figure 3d; e.g., Searle et al., 1997; Zhu, et al., 2005; Green, et al., 2008), around the Eocene/Oligocene boundary (e.g., 34 Ma; Aitchison, et al., 2007; Najman et al., 2010).

The rocks in the Muslim Bagh area can be broadly divided into: the passive margin, the Muslim Bagh Ophiolite, the Bagh Complex and the Flysch Zone (Figure 1). In the south, the tectonically lowermost zone is the Calcareous zone of the Indian passive continent margin and consists of Triassic to Paleocene limestones, sandstones, shales, marls and occasional conglomerates; these include the Bibai Formation of Campanian-Maastrichtian age (Kazmi, 1984), comprising volcanic conglomerate, lava flows and ash. The Calcareous Belt is thrusted over by the suture zone; lying between the Indian plate and Afghan Block (Gansser, 1964; Figure 1) and consists of the Muslim Bagh Ophiolite and Bagh Complex. The Muslim Bagh Ophiolite and Bagh Complex are described in detail below. The Flysch Belt, which comprises marl, shale, sandstone and conglomerate, lies to the north of the suture zone (Figure 1) and unconformably overlies the ophiolite (Kasi et al., 2012).

ACCEPTED MANUSCRIPT

3. Geology and petrography of the Muslim Bagh Ophiolite

The Muslim Bagh Ophiolite mainly comprises two massifs: the western Jang Tor Ghar Massif (JTGM) and the eastern Saplai Tor Ghar Massif (STGM) (Figure 1). The two blocks are belong to the same ophiolite nappe, and overlie subophiolitic mélange and sediments of the Bagh Complex (Mahmood et al., 1996; Naka et al., 1996; Figure 1). The JTGM is mainly composed of mantle rocks and covers ~150 km^2, whereas the STGM covers ~180 km^2 and consists of a near-complete ophiolitic sequence ranging from foliated peridotite at the base through the mantle–crust transition zone to crustal rocks at top (Figure 2). Numerous mafic dykes cross-cut the STGM at all structural levels. The ophiolite preserves a series of subophiolitic metamorphic rocks at the north-western side of the JTGM and at the west of STGM (Figure 1).

3.1. The metamorphic sole rocks

The metamorphic sole rocks beneath the Muslim Bagh Ophiolite consist of basal peridotite (part of the ophiolite) and sub-ophiolitic metamorphic rocks which display an inverted metamorphic sequence grading from garnet amphibolite facies, to amphibolite facies, to lower greenschist facies near the mélange contact. The sole rocks are likely to be a composite of rocks developed at different pressures and temperatures, at different times along a thrust plane, which were subsequently amalgamated into a single unit beneath the hot advancing ophiolitic crust (e.g., Lytwyn and Casey, 1995). The basal peridotite shows mylonitic textures formed in response to ductile lithospheric deformation during the initiation of intra-oceanic subduction (e.g., Nicolas, 1989; Mahmood et al., 1995), whereas going upward asthenospheric microstructures predominate. The foliation plane in the Jang Tor Ghar sole rocks strikes NE–SW and dips an

ACCEPTED MANUSCRIPT

average 50º towards the SE. The majority of the lineations display NE – E orientation and suggest E and NE thrusting initiated at temperatures between 900-1,000 °C (cf., Nicolas, 1989), forming mylonitic peridotite and continuing eventually downwards to high grade amphibolite conditions (Kakar, 2011).

3.2. The mantle section and the mantle-crust transition zone

The Muslim Bagh Ophiolite has a thick mantle section exposed in both massifs with a combined thickness of ~11 km (Siddiqui et al., 1996 and Figure 1). The mantle section of the Muslim Bagh Ophiolite is sub-divided into foliated peridotite and a mantle–crust transition zone. Both the sections have segregated bodies of chromitite.

The foliated peridotite, found in both ophiolite massifs, represents the upper mantle segment of oceanic lithosphere. Additionally, the STGM is also overlain by a dunite rich transition zone (Figures 2 and 3). Both massifs consist mostly of foliated, variably serpentinized harzburgite with minor dunite; however, lherzolite (or clinopyroxene-bearing harzburgite in the STGM) is also reported from the lower part of the massifs (Mahmood et al., 1995). The peridotites grade downward into basal peridotite; with a mylonitic-to-porphyroclastic texture characterized by prominent dunite/harzburgite compositional banding. Both areas have numerous chromite deposits and are intruded by mafic dyke swarms and gabbroic intrusions (Figure 1). In the peridotites, foliation and lineations are marked by elongated spinel and orthopyroxene grains. The dunite present in the mantle section is either interlayered with harzburgite, or occurs within the harzburgite as larger bodies with segregated podiform chromite deposits. The transition zone chromite bodies are larger in size and lower in grade compared to those found in the dunite of the lower foliated peridotite rocks of the mantle section.

ACCEPTED MANUSCRIPT

Petrographically, the rocks of the mantle section comprise lherzolite, harzburgite, , dunite, serpentinite, wehrlite and pyroxenite. The lherzolites are medium to coarse grained and porphyroclastic-to-mylonitic in texture with 70 %[1] olivine, 15–20 % orthopyroxene, 5–10 % clinopyroxene and 2 % spinel (Mahmood et al., 1995). Harzburgites are generally coarse grained and show autoclastic and hypidiomrophic granular textures in relatively fresh varieties, while a granoblastic texture predominates in altered rocks. The harzburgites are composed of 25–35 % orthopyroxene, 5-10 % olivine, 56-60 % serpentine and 3–6 % chromium spinel with ~2 % clinopyroxene (Siddiqui et al., 1996). The harzburgites in the upper part of the STGM are much more depleted in orthopyroxene (Siddiqui et al., 1996). The dunites are medium-coarse grained with a granoblastic texture comprising olivine (0-15 %) which is found as relict cores surrounded by a mesh of serpentine (75-80 %), antigorite and occasionally iddingsite. Clinopyroxene (2-3%), orthopyroxene (1-2 %) and spinel (2-3 %) comprise the rest of the rock (Siddiqui et al., 1996).

The 5-6 km thick mantle-crust transition zone of the Muslim Bagh Ophiolite is only exposed in the STGM and is characterized by a dunite sequence with minor chromite, wehrlite, pyroxenite and gabbro as discontinuous bands or lenses. A well-exposed transition zone south of Nisai (Figure 1) is rich in dunite and grades downwards into depleted harzburgite. The dunite is several hundred metres thick and is intruded by numerous dykes, sills and veins of gabbros, anorthosite and pyroxenite in its upper section near the base of the gabbro (Boudier and Nicolas, 1995; Mahmood et al., 1995).

3.3. The crustal section

[1] All mineralogical proportions are modal abundances

ACCEPTED MANUSCRIPT

The crustal section of the Muslim Bagh Ophiolite is exposed in the eastern portion of STGM (Figures 1-2) and is characterized by a cyclic sequence of ultramafic–mafic cumulates and a sheeted dyke complex.

3.3.1. Ultramafic–mafic cumulates

The mafic-ultramafic cumulate sequence is mainly composed of single or cyclic successions (Figure 2) each 200 to 1500 m thick (Salam and Ahmed, 1986). Each cycle typically has basal dunite grading upwards into wehrlite followed by clinopyroxenite, gabbro (Figure 2) and occasionally anorthosite at the top. Generally, the thickness of (occasionally layered or foliated) gabbros in individual cycles increases upwards (Figure 4a). Many small and medium-sized dolerite dykes (~1–3 m wide) have intruded the lower mafic-ultramafic cumulate sequence.

In the dunite, olivine (altered mostly to serpentine) occurs either, as subhedral or anhedral grains or, in irregular fractures filled with serpentine, chromite and magnetite. Some samples contain a few grains of enstatite and diopside. Wehrlite is medium to coarse grained with granular porphyritic, hypidiomorphic and occasional granoblastic textures. The wehrlite is comprised of anhedral granoblasts (~15%) of olivine (partially altered to antigorite) with large subhedral to euhedral grains of diopside (20-30 %). These crystals are surrounded by a mostly serpertinised groundmass (50-55 %) with a mesh texture containing small amounts of magnetite, spinel and enstatite. Pyroxenite is medium to coarse grained with a poikilitic to subpoikilitic texture and contains abundant diopside (90–95 %), with accessory amounts of orthopyroxene, olivine and opaque minerals with rare bytownite plagioclase.

At their base, the gabbroic rocks comprise olivine gabbro, gabbronorite and norite while hornblende-rich gabbro is common nearer the top of the sequence. The gabbroic rocks are

ACCEPTED MANUSCRIPT

melanocratic, holocrystalline, and medium to coarse grained (Figure 4b), with well-developed thin layering in some varieties. The norites and gabbronorites consist of 45–70 % plagioclase, 15–30 % clinopyroxene, 10–20 % orthopyroxene, with minor magnetite, ilmenite and secondary hornblende, tremolite, chlorite and sericite. Olivine gabbros contain up to 8 % olivine, and their plagioclase is more calcic (An_{70-72}) than the other gabbroic rocks of the crustal section. Hornblende-rich gabbros comprise 45–50 % labradorite, 30–40 % hornblende, 3–5 % augite, with minor olivine, magnetite and apatite.

3.3.2. The sheeted dyke complex

The ~1 km thick sheeted dyke complex crops out in the east of the STGM (Figure 1) (Sawada et al., 1992; Mahmood et al., 1995; Siddiqui et al., 1996; 2011). The dykes comprise dolerites, diorite and plagiogranites but have undergone greenschist and amphibolite facies metamorphism. The complex is rooted in the underlying gabbros and was emplaced over a protracted time period since the dykes range from highly foliated and mylonitizatised varieties that have undergone amphibolite metamorphism, through those that are discordant, weakly foliated and metamorphosed (amphibolite/greenschist facies), to intrusions without foliation and metamorphism that are discordant to foliation or layering.

The dykes range in thickness from 10–100 cm and generally strike between 140^{o} –160^{o} and dip 55^{o}, on average towards the northeast. Interestingly, sheeted dykes of the Muslim Bagh Ophiolite are less well-developed compared to those of other Tethyan ophiolites (e.g., Troodos; Varga, 2003) (Figure 4c). Petrographically, the dolerites consist of hornblende, ferro-hornblende, ferro-actinolite, ferro-tremolite, plagioclase and minor quartz (Figure 4d). Hornblende occurs as small prismatic euhedral to subhedral crystals while plagioclase (An_{12-54}) forms euhedral to

ACCEPTED MANUSCRIPT

subhedral and tabular crystals which often contain small grains of apatite, ilmenite, magnetite and hematite.

Plagiogranite is found as small dykes and inclusions (Figure 4e) in sheeted dykes and is granular and medium grained with micropegmatitic intergrowths between quartz and sodic plagioclase (Figure 4f). This rock comprises 43–50 % plagioclase, 8–20 % hornblende and 24–30 % quartz, with minor pyroxene, chlorite and opaques and accessory apatite and zircon.

3.4. The mafic dyke swarm

One of the striking features of the Muslim Bagh Ophiolite is the presence of numerous mafic dykes which crosscut almost the whole ophiolite and the metamorphic sole rocks. Individual dykes range in thickness from a metre to tens of metres and extend along strike up to 10 km (Figures 1-2). The dykes strike 140° to 170° and are abundant in the STGM with a few dykes found on the western side of the JTGM. The trend of the mafic dyke swarm is parallel to that of the sheeted dyke complex (Figure 1), suggesting that they were emplaced parallel to the ridge during, or soon after, ophiolite obduction. The dykes possess chilled margins and have thermally metamorphosed their immediate country rocks. Field observations reveal that these dykes appear to feed a few small magma chambers (gabbroic plutons). At the base of these gabbro plutons a transition zone has developed between the top of dykes and the base of the gabbro (Khan et al., 2007). Petrographically, dolerites are medium to fine grained, often showing ophitic texture with 15–30 % pyroxene (augite and pigeonite) crystals and 55–60 % plagioclase (An_{62}) laths (variably sericitised) with opaques and secondary minerals.

4. Geology and petrography of the Bagh Complex

ACCEPTED MANUSCRIPT

The Bagh Complex is a tectonic mélange (Ahmad and Abbas, 1979) which Naka et al. (1996) on the basis of lithology, age and structural similarities correlated with similar complexes, found beneath the Semail Ophiolite of Oman (e.g., Robertson and Searle, 1990; Bernoulli, et al., 1990). The Bagh Complex is in thrusted contact with the overlying Muslim Bagh Ophiolite (Figure 1) and this contact is commonly marked by a serpentinite and mudstone mélange. Following Mengal et al. (1994) the Bagh Complex is divided into a mélange unit, a basalt-chert unit, a hyaloclastite-mudstone unit, and a sedimentary unit (Figure 1) with each unit forming an individual thrust sheet.

The mélange unit (~100-500 m thick) consists of serpentinite mélange near the thrust contact with ophiolite (Figure 1) and is underlain by a mudstone mélange. The serpentinite mélange includes blocks of ultramafic-mafic rocks, metamorphic rocks and sedimentary rocks in a serpentinite matrix. The ultramafic-mafic rocks are likely to be derived from the Muslim Bagh Ophiolite along with basalt and sedimentary rocks from the Bagh Complex. The mudstone mélange includes basalt, radiolarian chert, limestone and shale blocks surrounded by mudstone and are most likely derived from the basalt-chert unit and the sedimentary unit in the Bagh Complex. Similar mélange units are found beneath other Tethyan ophiolites (e.g., Polat and Casey, 1995; Polat et al., 1996).

The basalt-chert unit (Bbc) of the Bagh Complex (Figure 1) was previously regarded to be the upper basaltic member of the Muslim Bagh Ophiolite (Ahmad and Abbas, 1979). The unit is characterized by predominantly pillowed basaltic rocks and volcanic breccias with bedded chert (containing radiolarian fossils spanning the whole Cretaceous period; Kojima et al., 1994), micritic limestone and hemi-pelagic mudstone. The unit is faulted and sheared but Mengal et al. (1994) have proposed that the basaltic rocks originally comprised the lower part of the unit and

ACCEPTED MANUSCRIPT

were overlain by limestone-chert and siliceous shale. The basalts of this unit are hypocrystalline, sub-porphyritic to sub-intersertal in texture, with plagioclase, augite, minor chlorite and ilmenite along with secondary actinolite and epidote. Some basalts contain hornblende phenocrysts and devitrified glass in the groundmass.

The hyaloclastite-mudstone unit (Bhm) consists of thick pillowed basalt and massive basanite, alkali basalt, tephrite and trachy-basalt that also occur as hyaloclastite and reworked volcanic breccias. These volcanic rocks are interbedded with mudstone, limestone and shale in the upper-middle part of the unit and are in places intruded by basalt and dolerite. Radiolarian assemblages from lower part of this unit yield an Early Cretaceous age (Kojima et al., 1994). The basanite and alkali basalt contain phenocrysts of hornblende and augite set in a groundmass of plagioclase, pargasite, phlogopite, opaques and glassy material. In the tephrite and trachybasalt phenocrysts of plagioclase, augite, olivine, pargasite and phlogopite are embedded in the groundmass of plagioclase with Ti-augite, pargasite, phlogopite, apatite, ilmenite and devitrified glass.

The rocks of the sedimentary unit (Bs) are Triassic–Jurassic in age i.e., slightly older than the two volcanic units. These sediments consist of limestone with alternating beds of mudstone, mudstone, sandstone, and conglomerate and are considered an integral part of the Calcareous Zone / Indian passive margin (Manan, 2013; Figure 1).

The Bagh Complex is in thrusted contact with both the Muslim Bagh Ophiolite and the Calcareous Belt to the south (Figure 1). Both these thrusted contacts strike NE-SW, dip steeply, and are consistent with the attitude of bedding in the Bagh Complex. This similarity implies that the boundary fault was originally nearly horizontal and was later folded during the deformation event that was also responsible for folding the Bagh Complex (Ahmad and Abbas, 1979; Otsuki,

ACCEPTED MANUSCRIPT

et al., 1989). All the units within the Bagh Complex are bounded by north-dipping thrust faults (Figure 1).

5. Geochemistry

5.1.Analytical methods

Samples were collected for analyses from each of the major igneous units, (approximate sample locations are given on Figure 2 and detailed information on each sample are given in Online Appendix 1) Following removal of weathered surfaces the samples were crushed in a steel jaw crusher and powdered using an agate Tema mill at Cardiff University. Two grams of sample powder were then heated in a porcelain crucible to 900 °C for 2 hours to determine loss on ignition. Major and trace elements were analysed using a JY Horiba Ultima 2 inductively coupled plasma optical emission spectrometer (ICP-OES) and a Thermo X7 series inductively coupled plasma mass spectrometer (ICP-MS) at Cardiff University, Wales.

The ignited powders were prepared for analysis by fusion of 0.1 g of sample with 0.4 g of lithium tetraborate flux in a platinum crucible on a Claisse Fluxy automated fusion system. The mixture was then dissolved in 30 ml of 10% HNO_3 and 20 ml of de-ionised water. After the sample was fully dissolved, 1 ml of 100 ppm Rh spike was added and the solution was made up to 100 ml with de-ionised water. ~20 ml of this solution was run on the ICP-OES to obtain the major element abundances. 1 ml of the solution was added to 1 ml of Tl and 8 ml of 2% HNO_3 and analysed on the ICP-MS to obtain the trace element abundances. Accuracy and precision of the data were assessed using the international reference materials NIM-G, JB-1A and BIR-1 (Online Appendix 2). The full data set can be found in Online Appendix 3 with a representative data set in Table 1.

ACCEPTED MANUSCRIPT

Nine samples: sheeted dykes (1), plagiogranite (1), mafic dyke swarm (3), gabbros (2), basalt Bbc (1) and basalt Bhm (1); were analysed for Sm–Nd and Rb–Sr isotopes. Samples were crushed in a stainless steel jaw crusher after removal of weathered rims. A split was ground to <2 mm grain size in a tungsten carbide ring mill. Following dissolution in Teflon bombs and column separation by ion exchange, $^{143}Nd/^{144}Nd$ and $^{87}Sr/^{86}Sr$ isotope ratios and Nd and Sm concentrations (by isotope dilution) were measured at Geology and Geophysics at the University of Adelaide, on the Finnigan MAT 262 TIMS in multi-dynamic mode. Methods used in the Adelaide laboratories have been described in detail by Elburg et al. (2003) and more recently by Payne et al., (2006). During the interval over which analysis was undertaken the in-house Nd standard (J and M specpure Nd_2O_3) gave 0.511604 ± 9. The La Jolla standard gave 0.511842 ±15 and BCR-1 yielded 0.512636 ±16. Blanks are in the order of 100-300 pg for Nd and < 200pg for Sm. All samples used for Sm–Nd analyses were spiked with mixed $^{149}Sm–^{150}Nd$ spike. Reproducibility of the $^{147}Sm/^{144}Nd$ ratio was better than 0.8%. The average $^{87}Sr/^{86}Sr$ ratio for SRM987 during the period when the samples were run was 0.710278 ±26 (2σ, n=45). Whole procedure blanks for Sr are better than 1 ng.

5.2. Alteration and element mobility

As has already been noted, the rocks of the complex are variably metamorphosed to greenschist-amphibolite facies and have undergone a substantial degree of hydrothermal alteration. These processes have invariably mobilised the large-ion lithophile elements and most of the major elements leading to considerable scatter on geochemical diagrams involving these elements and oxides. Consequently, these more-mobile elements have been excluded from the following discussion in favour of elements generally regarded to be relatively immobile (e.g.,

ACCEPTED MANUSCRIPT

Winchester and Floyd 1976; Pearce, 1982; Pearce 1996; Hastie et al., 2007) under the hydrothermal and metamorphic conditions experienced by these rocks (i.e., the high-field strength elements and the rare earth elements).

5.3. Gabbros

The gabbros range in MgO content from 3.7-14.4 wt.% with most in the range 7.5-9.5 wt.% MgO (Figure 5). This variability is also borne out by the Co vs. Th and Nb/Y vs. Zr/Ti classification diagrams (Figure 6a-b). On the Co-Th diagram, the gabbros range from basaltic to dacitic-rhyolitic compositions in terms of their Co contents, and while most of the gabbros have Th contents consistent with an island arc tholeiite (IAT) signature, several gabbros (C47A; C34) have elevated Th contents suggestive of a more calc-alkaline signature. The samples display less scatter on Figure 6b with all of the samples plotting in the basaltic field with the exception of one sample that classifies as a basaltic andesite. Sc, Zr, TiO_2, and Th (along with Hf, Al_2O_3, Y and Sr – not shown) broadly increase with decreasing MgO (Figure 5), whereas Co (Figure 5c), V, Ni, Cr decrease with increasing MgO. All the remaining relatively immobile elements, including the REE do not correlate with MgO contents (e.g., Figure 5c).

Although most of the chondrite-normalised REE patterns of the gabbros are broadly flat, several samples (C47A; C34) have a more-enriched light (L)REE signature and C191 has a depleted LREE signature (Figure 7c). All the Muslim Bagh gabbros have a flat heavy (H)REE pattern, and several samples have slight positive Eu anomalies. N-MORB-normalised incompatible trace element patterns show most of the same features and additionally reveal that all samples possess a negative Nb-Ta anomaly (Figure 8).

ACCEPTED MANUSCRIPT

In terms of ratio:ratio trace element diagrams (Figure 9) the gabbros appear to be derived from a broadly MORB-like source region with a subduction input (Figure 9d). The Dy/Yb vs. Dy/Dy* diagram (Figure 9c) also appears to indicate a role for amphibole in the crystal fractionation/accumulation history of these gabbros.

5.4. Sheeted dyke complex including the plagiogranites

The sheeted dykes span a relatively narrow range in MgO content from 4.8-6.9 wt.% , whereas the plagiogranites all contain <0.6 wt.% MgO (Figure 5). On the Co-Th classification diagram (Figure 6a) the sheeted dykes range from basaltic to dacitic-rhyolitic compositions with all but two of the samples (C43; C52) having a calc-alkaline signature. Like the gabbros, the sheeted dykes display less scatter on the Nb/Y vs. Zr/Ti classification diagram, as opposed to the Co-Th diagram, with all of the samples plotting in a tight field straddling the basalt/basaltic andesite boundary (Figure 6b). Unsurprisingly, the plagiogranites mostly plot in the dacite-rhyolite fields on both classification diagrams (Figure 6). The sheeted dykes generally have more coherent trends than the gabbros when plotted against MgO (Figure 5), with La, Zr, TiO_2, Th and Co (along with Hf, V, Y, Nb and the REE – not shown) broadly increasing with decreasing MgO, whereas Sc and Al_2O_3 (not shown) decrease with increasing MgO. The plagiogranites have generally low trace element contents (Figure 5).

With the exception of C43 (the least evolved sample) chondrite-normalised REE patterns of the sheeted dykes form a reasonably coherent group with near-parallel LREE-enriched and flat HREE patterns (Figure 7b). Several samples have slight negative Eu anomalies. N-MORB-normalised incompatible trace element patterns have essentially flat HREE and HFSE patterns with variable negative Nb-Ta and Ti anomalies (Figure 8b). This, and the evidence from

ACCEPTED MANUSCRIPT

ratio:ratio diagrams, indicates that the sheeted dykes are derived from a broadly MORB-like source region with a subduction input. The plagiogranites have chondrite-normalised REE patterns that vary from one sample with a flat pattern and a negative Eu anomaly (C37), through to several LREE enriched (La_n/Sm_n ~7) samples (C136; C35) with flat HREE patterns (~2-3 x chondrite) and positive Eu anomalies (Figure 7d). Like the sheeted dykes, all the plagiogranites have negative Nb-Ta and Ti anomalies on an N-MORB- normalised diagram (Figure 8d).

5.5. Mafic dyke swarm

The mafic dyke swarm range in MgO content from 4.3-8.0 wt.% (Figure 5). On the Co-Th classification diagram (Figure 6a) all the samples (with the exception of the most evolved dyke, C26, which plots as a dacite) classify as island arc tholeiite basalts. The mafic dykes form a coherent group on Figure 6b with all of the samples (except C30) lying in the basalt field. The dykes generally show coherent trends when plotted against MgO, with La, Zr, TiO_2, and Th (along with Hf, V, Y, Nb and the other REE – not shown) broadly increasing with decreasing MgO, whereas Sc, Cr, Ni (Figure 5) and Al_2O_3 (not shown) decrease with increasing MgO.

Chondrite-normalised REE patterns of the mafic dyke swarm are flat to slightly LREE-depleted, with some samples having a very slight negative Eu anomaly (Figure 7a). N-MORB-normalised incompatible trace element patterns show flat N-MORB-like patterns and although all the samples possess a negative Nb-Ta anomaly this is much less marked than in the sheeted dykes (Figure 8a). Figure 9 indicates that the rocks of the mafic dyke swarm are derived from a MORB-like source region probably with less of a subduction influence than either the gabbros or sheeted dykes. The Dy/Yb vs. Dy/Dy* diagram may also indicate a limited role for amphibole fractionation in their petrogenesis (Figure 9c).

ACCEPTED MANUSCRIPT

5.6. Lavas of the Bagh Complex

On the basis of their geochemistry the lavas of the Bagh Complex can be divided into: a tholeiitic, MORB-like type found only in the basalt-chert unit and alkalic, ocean island basalt (OIB)-like type found in the hyaloclastite-mudstone unit (Figure 6b)

The MORB-like and OIB-like lavas range in MgO contents from 2.3-8.2 wt.% and 5.7-11.6 wt.% respectively (Figure 5). On the Co-Th diagram all but the most evolved MORB-like lava (C62; an andesite) are classified as basalts (Figure 6a) and on the Nb/Y vs. Zr/Ti diagram all plot as basalts (Figure 6b). The tholeiitic- alkalic nature of the two groups is clearly borne out on Figure 6b.

These two groups are also very evident on MgO variation diagrams, particularly for the most incompatible elements, although there are no coherent fractionation trends for these incompatible trace elements for either the MORB-like or the OIB-like types (Figure 5). Clearer fractionation trends are however observed for the compatible elements, e.g., Sc (along with Ni and V – not shown).

The chondrite-normalised REE patterns of the OIB-like lavas are enriched in the LREE and depleted in the HREE (Figure 7e) and plot slightly above the enriched end of the tramlines on Figure 9b. These lavas also plot within and slightly below the Iceland (plume) array on Figure 9a. With the exception of sample C83 the more-depleted Bbc lavas have LREE-depleted and flat HREE patterns. Sample C83 has moderately-enriched LREE with flat HREE patterns (Figure 8e). On Figure 9a all the depleted samples (except C83, which plots in the plume array) plot below the lower tramline in the field of present-day MORB. On Figure 9c the enriched samples lie in the OIB field while the more depleted samples have MORB-like signatures.

ACCEPTED MANUSCRIPT

Significantly, the N-MORB- normalised incompatible trace element patterns also reveal that all but one of the samples (in both groups) possess a negative Nb anomaly and, for most samples, a negative Ta anomaly (Figs.8e-f). The most pronounced negative Nb-Ta signatures occur in the MORB-like samples. Most of the samples in these two groups plot above the MORB-OIB array in Figure 9b indicating elevated Th in their source region.

5.7. Sr and Nd isotopes

A small subset of samples have been analysed for Nd and Sr isotopes (Figure 6c). However, given the extent of sub-solidus hydrothermal alteration and metamorphism that the samples have undergone it is likely that the Sr isotope systematics in these samples have been disturbed and so do not represent magmatic values and this is borne out by the elevated age-corrected $^{87}Sr/^{86}Sr$ of some of the samples and so Sr isotope values will not be considered further.

The rocks of the Muslim Bagh Ophiolite range in $(\varepsilon_{Nd})_i$ from +7.5 to +3.2, with the mafic dyke swarm generally having the highest values (Figure 6c), in keeping with their more depleted LREE patterns, while the gabbros have broadly lower values. The analysed Bbc sample has a MORB-like LREE signature and a $(\varepsilon_{Nd})_i$ of +5.8 that falls within the more-enriched end of the MORB array , while and OIB-like Bhm sample has and $(\varepsilon_{Nd})_i$ of +3.9 (Figure 6c)

6. Discussion

6.1. The nature and composition of mantle section

ACCEPTED MANUSCRIPT

The Muslim Bagh mantle section is dominated by foliated harzburgite with subordinate dunite. Such harzburgitic mantle sections of ophiolitic complexes have often been explained as depleted peridotite resulting from large degrees of partial melting of a lherzolite source (e.g., Nicolas, 1989; Baker and Beckett, 1999). This harzburgite may also be affected by magma–mantle interaction involving precipitation of orthopyroxene and olivine (e.g., Kelemen et al., 1992). Petrographically, the Muslim Bagh harzburgites are porphyritic with low modal clinopyroxene and the dunites are also poor in pyroxene, indicating that they are residual after significant melting. The deformed relict primary minerals and the irregular shape of the spinel grains in the peridotite further indicate residual mantle that has undergone high-temperature deformation under upper mantle plastic flow conditions (e.g., Nicolas, 1989; Mahmood et al., 1995; O'Hara et al., 2002).

Experimental studies on peridotite show that progressive melting of lherzolite rapidly eliminates clinopyroxene and gradually reduces the proportion of orthopyroxene (Mysen and Kushiro, 1977; Jaques and Green, 1980). As melting proceeds, forsterite and NiO contents of olivine, Mg# of pyroxene, and Cr # of spinel increase, and Al_2O_3 contents of the residual spinel and pyroxene and of the whole rock decrease (Dick and Bullen, 1984; O'Hara et al., 2002). The Muslim Bagh mantle rocks possess higher Cr# and Mg# in accessory spinel and orthopyroxene, thus implying that they are the result of a high-degree of partial melting of a depleted mantle source (Siddiqui et al., 1996; Arif and Jan, 2006). All these features indicate a residual upper mantle origin or a higher degree of partial melting (30-45%) of a depleted mantle source, for the Muslim Bagh peridotite (cf., Dick and Fisher, 1984).

The origin and petrogenesis of the transition zone in ophiolites has also been widely debated, with some advocating an origin by olivine fractionation and accumulation from picritic

ACCEPTED MANUSCRIPT

magma (e.g., Coleman, 1977; Malpas, 1978; Elthon et al., 1982), while others propose a residual mantle origin (e.g., Nicolas and Prinzhofer, 1983; Boudier and Nicolas, 1995; Kelemen et al., 1995; and Zhou et al., 1996). More recently Suhr et al. (2003) and Zhou et al. (2005) have suggested that the transition zone formed by processes of mantle-melt reaction and proposed it was an integral part of the mantle sequence.

Although in the Muslim Bagh Ophiolite the characteristics of some of the dunite especially in the uppermost part of the transition zone is more supportive of a cumulate origin as proposed by Siddiqui et al.(1996), no cumulates have been found in most of the transition zone dunites. The presence of clinopyroxene and plagioclase in the uppermost part of the transition zone is probably the result of magmatic impregnation and so could represent a crystal-melt mixture, and the lenses and dykes/sills of gabbros may have been injected laterally due to compaction (e.g., Benn et al., 1988). Therefore, the uppermost cumulate part of transition-zone dunite in the Muslim Bagh is likely to have formed by crystal fractionation from crustal magma chambers during the first stages of crystallization, (e.g., Malpas, 1978), whereas the textures in lower part of the transition-zone are more indicative of high degrees of partial melting and extensive melt–rock interaction (e.g., Nicolas and Prinzhofer, 1983; Suhr et al., 2003; Zhou et al., 2005). In contrast, Siddiqui et al. (1996), proposed that the dunite rich transition zone between the residual mantle and crustal rocks was composed completely of ultramafic cumulates. However, our detailed field and petrographic work has revealed that the lower reaches of transition zone show no evidence of cumulate textures and are, at least in part, the products of mantle-melt reaction.

6.2. Petrogenesis of the crustal rocks

ACCEPTED MANUSCRIPT

The crustal part of the Muslim Bagh Ophiolite comprises a cyclic succession of ultramafic-mafic cumulates. Each cycle differs in its lithological thickness and sequential arrangement and this is likely to be due to the different timing of crystallization of cumulus minerals resulting from the supply rate of magma to the chamber. Most of the Muslim Bagh gabbros are tholeiitic in nature, although a few have a distinct calc-alkaline signature (Figure 6a), and contain both cumulus and non-cumulus phases, with olivine, pyroxene and plagioclase all involved in the fractionation processes. This is borne out by the whole-rock geochemical range from basaltic-dacitic compositions and the slight positive Eu anomaly observed in some samples (Figure 7a). The lack of correlation of MgO with many incompatible elements (e.g., Figure 5) is likely to be a reflection of the cumulate nature of many of the gabbros. Furthermore, although not obvious from the petrography, the Dy/Lu vs. Dy/Dy* diagram also suggests that amphibole fractionation/accumulation played a significant role in the crystallisation history of these rocks. This indicates that the magmas were 'wet' and this, in conjunction with their negative Nb-Ta anomaly (Figure 8c), suggests formation in a supra-subduction zone. Based on a much smaller data set on a restricted range of elements Siddiqui et al. (1996) interpreted this ophiolite to have formed in a back arc basin, however, our geochemical data is more consistent with formation in a supra-subduction zone. Although the mantle source region of the gabbros is broadly MORB-like there is some evidence from the $(Ce/Ce^*)_{Nd}$ vs. Th/La diagram for a subduction component derived from continental detritus, suggesting proximity to a continental margin.

The Muslim Bagh Ophiolite has a well-developed cyclic repetition of ultramafic to mafic rocks at the base with a relatively less well-developed, more-evolved cumulate crustal section. These features are characteristic of gabbros that form in a slow to ultra-slow-spreading environment and indicate that the rocks may have formed over differing lengths of time as a

ACCEPTED MANUSCRIPT

result of a low magma supply in pulses (e.g., Cannat et al., 1995, 2006; Nicolas et al., 1999; Michael, et al., 2003).

The configuration of the crustal section with a poorly developed sheeted dyke complex and well-developed plutonic sequence (Figure 2) also indicates that these sheeted dykes are formed in a tectonic setting with a slow spreading rate. Our field and petrographic observations from the Muslim Bagh Ophiolite support the proposal of Robinson et al. (2008) that well-developed sheeted dyke complexes are uncommon in supra-subduction zone environments because the spreading rate and magma supply rate are rarely balanced.

Like the gabbros, the sheeted dykes are tholeiitic to calc-alkaline in nature and their much more coherent trends (than the gabbros) on element vs. MgO diagrams reflects the significant role played by fractionation (olivine, clinopyroxene and possibly amphibole; Figures 5a-b, e, 9b) in their petrogenesis. Again, similar to the gabbros, the source region of the sheeted dykes is broadly MORB-like with a subduction input (Figure 8b). As noted above, the Muslim Bagh plagiogranites are found both at the top of the gabbro plutons and in the sheeted dykes and they also possess a tholeiitic to calc-alkaline signature. The highly variable trace element signature of the plagiogranites (Figure 8d) suggests that either they represent highly fractionated magma chamber differentiates (i.e., those samples with negative Eu anomalies indication plagioclase fractionation) or late stage crystal (plagioclase) cumulates (i.e., the samples with positive Eu anomalies implying plagioclase accumulation). Alternatively, the plagiogranites may be the result of hydrous partial melting of oceanic gabbros as proposed by Koepke et al. (2004; 2007). Although the low TiO_2 content of the Muslim Bagh plagiogranites (Figures 5b and 8d) is consistent with an origin by partial melting of altered (hydrous) gabbro (Koepke et al. 2007), their variable Eu anomalies (positive and negative) are more difficult to reconcile with this

ACCEPTED MANUSCRIPT

model. Further speculation on the origin of plagiogranite is beyond the scope of this paper, however, the subduction-related signature of the Muslim Bagh plagiogranites and their intimate association with both the gabbros and the sheeted dykes strongly indicates a co-genetic relationship.

Khan et al. (2007) proposed that the later mafic dyke swarm were subduction related. However, our study indicates that these dykes represent a later intrusion event are geochemically distinctive from the rest of the Muslim Bagh Ophiolite, in that they are tholeiitic and have generally much flatter to slightly LREE-depleted REE patterns. Additionally, the mafic dyke swarm has much less-pronounced negative Nb-Ta anomalies than the rest of the complex (Figure 8a). All these features in conjunction with the evidence from Figure 9b indicate that the mafic dyke swarm have a less-marked subduction signature than, particularly, the sheeted dykes. This weaker subduction signature is also reflected in the lower $(\varepsilon_{Nd})_i$ values of the mafic dyke swarm rocks (Figure 6c). Contrary to the model of Khan et al. (2007) these features imply that the dykes formed further from the supra-subduction zone than the rest of the complex and may have risen through a slab-window (Figure 10e; cf., Lytwyn and Casey, 1995; Dilek et al., 1999; Celik, 2007; Xu, et al., 2008).

6.3. Tectonic setting and petrogenesis of the Bagh Complex basaltic rocks

As reviewed in Section 2, paleontological evidence indicates that the basaltic rocks of the Bagh Complex are generally older (Early–Late Cretaceous; Sawada et al., 1992; Kojima et al., 1994) than the Muslim Bagh Ophiolite suite (80.2 ± 1.5 Ma; Kakar et al., 2012) and so cannot be regarded as part of the ophiolite as proposed by Khan et al. (2007). Siddiqui et al. (1996)

ACCEPTED MANUSCRIPT

proposed that these rocks formed in the same back-arc basin as the rest of the ophiolite, however, the geochemistry of the Bagh Complex lavas and their older age makes this improbable.

The rocks of the Bagh Complex are distinctive in terms of their geochemistry, with both tholeiitic MORB-like signatures (in the basalt-chert unit) and alkalic OIB-like signatures (in the hyaloclastite-mudstone unit) (e.g., Figure 8e-f). It is likely that the tholeiitic rocks represent Neo-Tethyan ocean floor, formed during the Cretaceous (Kojima et al., 1994), after the breakup of Gondwana, and although only one of these samples was analysed for isotopes, the MORB-like $(\varepsilon_{Nd})_i$ of +5.8 supports this assertion. However, the rocks are not as depleted in LREE as N-MORB (Figure 8e) and have negative Nb-Ta anomalies, the significance of which will be discussed below. The OIB-like volcanics that comprise significant exposures of basalts in Bagh Complex have been neglected in models of the tectonic setting of Muslim Bagh Ophiolite Complex by previous workers (e.g., Siddiqui et al., 1996 and Khan et al., 2007). These alkaline rocks are clearly a result of a relatively small degree of mantle melting in the garnet-lherzolite stability zone (>60km), so it is likely that melting occurred off-axis below relatively thick oceanic lithosphere. This evidence suggests that these rocks are most likely to have formed by melting of a hotspot-derived source region during Middle–Late Cretaceous. The high-MgO contents (>10 wt.%) of some of the OIB-like lavas also supports a hotspot source as does the fact that the samples plot within or slightly below the Iceland (plume) array on Figure 9a. Furthermore, the occurrence of other Cretaceous hotspot-derived lavas and intrusions in the accreted Tethyan sequences of the region (e.g., Sawada et al., 1992; Mahoney et al., 2002; Kerr et al., 2010) also lends support to a mantle plume origin for the OIB-type lavas in this study. It should also be remembered that the Cretaceous represents one of the most intense periods of

ACCEPTED MANUSCRIPT

mantle plume-related volcanism over the last 250 m.y. particularly in the oceans (e.g., Kerr, 2014).

Somewhat enigmatically, for magmatic rocks that all the evidence suggests formed in an ocean basin, most of the OIB-like and MORB-like lavas of the Bagh Complex possess negative Nb (and Ta) anomalies on an N-MORB normalised diagram. This implies that these rocks either contain a subduction component or continental crust. In an oceanic setting the simplest way to impart a negative Nb-Ta anomaly to a suite of magmatic rocks is to introduce the component into the upper asthenosphere by subduction (i.e., by the release of Nb-Ta depleted fluids from a descending slab); however the problem with this mechanism for the rocks of the Bagh Complex lies in the fact that both shallow-derived MORB-like lavas and the deep mantle plume-derived OIB-like lavas show this signature. It is difficult to envisage how contamination of the upper asthenosphere with a subduction-derived fluid could substantially modify the composition of a mantle plume that probably originates from at least the 660km discontinuity, and possibly the core-mantle boundary.

Alternatively, it is possible that substantial fragments of continental crust were incorporated into the Tethyan ocean basin during the breakup of Gondwana. We envisage that this could have occurred in a manner similar to what has been proposed for the similarly-aged lavas of the Kerguelen Plateau in the Indian Ocean that are contaminated with continental crust from fragments incorporated during Gondwana continental break-up (e.g., Frey et al. 2002). Continental fragments, if incorporated into the opening Tethyan oceanic basin during break-up could have contaminated both the MORB- and OIB-like basalts preserved in the Bagh Complex and we would contend is a more plausible explanation than a subduction-derived component in

ACCEPTED MANUSCRIPT

the upper asthenosphere, which can only really explain the Nb-Ta depletion in the MORB-like rocks.

6.4 Comparison of Muslim Bagh Ophiolite with Bela and Waziristan Ophiolites

There are several similarities as well as differences between the Muslim Bagh Ophiolite and the other ophiolites of the western Indian suture such as Waziristan and Bela ophiolites. The Waziristan Ophiolite, located north of the Muslim Bagh Ophiolite (Figure 1) is highly dismembered and consists of three main nappes, from east to west these are: the Vezhda Sar Nappe, comprised only of pillow basalts; the Boya Nappe, made up of accretionary wedge and mélange with ultramafic and gabbroic rocks that are irregularly distributed as fault-bounded blocks within a larger mass of pillow basalt; and the Datta Khel Nappe, mostly comprising sheeted dykes with smaller proportions of other components such as gabbros and pillow basalts (Khan, S-R, 2000). Faunal evidence suggests that the ophiolite is of Tithonian-Valanginian age (151-136 Ma). It was thrust over the Mesozoic shelf-slope sediments of the Indian Plate to the east during the Paleocene and is unconformably overlain by sedimentary rocks of Early to Middle Eocene age to the west (Beck et al., 1995; Khan S-R et al., 2007).

The Bela Ophiolite is located south of the Muslim Bagh Ophiolite (Figure 1) and is the largest outcrop of the oceanic lithosphere in the western suture zone. The Bela Ophiolite is divided into two sub units; the Bela Ophiolite suite; and the lower Subduction-Accretion Complex. The dismembered Bela Ophiolite suite can be reconstructed into one single thrust sheet and consists of peridotite and sheeted dykes and small outcrops of basalts (Khan, 1999). The ophiolite unit records ^{40}Ar–^{39}Ar magmatic ages of 70-68 Ma and emplacement ages of 66-64 Ma (Gnos et al., 1998; Xiong, et al., 2011). The lower unit of accretionary wedge-trench

ACCEPTED MANUSCRIPT

sediments consists of imbricated sheets of 50 to 1500 m thick and half a kilometre long. Each imbricate sheet contains a complete or partial sequence of oceanic ridge-related pillow lavas with geochemical signature of E-MORB (Gnos et al., 1998) that is covered by pelagic to hemi pelagic cherts, shales and limestones that are intruded by doleritic dykes. These sediments contain fossils of Aptian to Lower Maastrichtian age (Sarwar, 1992; Xiong, et al., 2011).

These three Tethyan ophiolite complexes each consist of an ophiolite suite and an underlying subduction-accretion complex (Khan, 1999; Khan S-R, 2000; Khan et al., 2007). The ophiolite sequence (upper units) of these ophiolites have geochemical signatures of an island arc implying a supra-subduction zone tectonic setting, and are considered to represent the western extension of Spontang Ophiolite that formed in the Neo-Tethys ocean 80-70 Ma and was then emplaced on the continental margin between 70-65 Ma (Corfield et al., 2001; Khan et al., 2009; Kakar et al., 2012).

6.5. New model for the origin and emplacement of Muslim Bagh Ophiolite

In the Middle Jurassic the northwestern margin of the Indian and Afro-Arabian plates began to rift apart (e.g., Ali, and Aitchison, 2008; Figure 10a). Continued spreading resulted in a narrow sea, or a branch of Tethys, that gradually widened up to the end of the Jurassic (e.g., Naka et al., 1996; Ali, and Aitchison, 2005, 2008). The Bbc unit represents the Neo-Tethyan ocean floor that formed along mid-Tethyan ridge near the northern and northwestern continental slope of the Indian plate (Kojima et al., 1994; Siddiqui et al., 1996; Figure 10b). The intra-plate alkali basalts within the Bagh Complex erupted in the mid-late Cretaceous when Neo-Tethyan oceanic lithosphere passed over a hotspot, possibly Réunion (e.g., Sawada et al., 1992; Mahoney

ACCEPTED MANUSCRIPT

et al., 2002; Kerr et al., 2010; Figure 10b-c). Many of these oceanic basalts are apparently contaminated with continental crust, possibly present as rafted blocks that were trapped within the oceanic lithosphere during the Jurassic rifting event (cf., Frey et al. 2002).

The oceanic lithosphere that ultimately was to become the Muslim Bagh Ophiolite formed ~80 Ma (Kakar et al., 2012) in a supra-subduction zone tectonic setting related to the west or northwest dipping subduction of a narrow branch of Neo-Tethyan ocean and the formation of a nascent arc (Gnos et al., 1997; Kakar et al., 2012; Figure 10c), followed by subduction rollback due to splitting of the nascent arc (Figure 10d) in a manner similar to that proposed by Dilek and Flower (2003) and Flower and Dilek (2003) further west in the Tethyan ocean. The formation of a metamorphic sole and initial intra-oceanic detachment/obduction of ophiolite due to extension in the nascent arc and slab rollback (Shervais, 2001; Flower and Dilek, 2003) was followed by the intrusion of mafic dykes (from a depleted mantle source) into both the metamorphic sole and the mantle section of the ophiolite. These off-axis magmas are likely have risen through a slab window (Figure 10e; cf., Lytwyn and Casey, 1995; Dilek et al., 1999; Celik, 2007; Xu, et al., 2008). The rocks of the mafic dyke swarm therefore exhibit a much weaker geochemical subduction signature than the rest of the Muslim Bagh rocks due to partial melting of a depleted source. Furthermore, this limited subduction signature also indicates that these dykes are genetically unrelated to the crustal mafic-ultramafic cumulates of the Muslim Bagh Ophiolite as proposed in the model of Khan et al. (2007).

The Indian plate continued to move northwards with the accretion of mélange between the Muslim Bagh Ophiolite and the Eurasian continental margin (Figure 10f). According to Mahmood et al. (1995), the Muslim Bagh Ophiolite was transported on the margin of the Indian continental plate during closure of Neo-Tethys until collision with the Eurasian continental plate.

ACCEPTED MANUSCRIPT

At this time (50-35Ma) the Muslim Bagh Ophiolite was obducted over the Indian Platform along with underlying Bagh Complex (Naka et al., 1996; Searle et al., 1997; Zhu, et al., 2005; Green, et al., 2008; Aitchison, et al., 2007; Najman et al., 2010; Figure 10f). Finally, the ophiolite was overlain by unconformable Early–Middle Eocene shallow marine strata (Allemann, 1979; Beck et al., 1995; Figure 10g). These shallow marine strata of the Nisai Formation along with immature turbidites of the Khojak Formation (Figure 1) were deposited in the Katawaz Basin; a narrow basin and a remnant Neo-Tethyan ocean which existed until the late Oligocene (Qayyum et al., 1996, 1997).

7. Conclusions

1. The Muslim Bagh Ophiolite has a thick residual mantle section with characteristics consistent with formation in a supra-subduction zone setting.

2. The Muslim Bagh Ophiolite crustal sequence comprises a well-developed cyclic succession of ultramafic to mafic rocks at the base with a less well-developed, more evolved crustal cumulate section. This crustal sequence is interpreted to have formed over differing lengths of time as a result of a low magma supply rate in pulses, probably in a slow to ultra-slow spreading environment. The gabbros are derived from a MORB-like mantle source region and a negative Nb-Ta anomaly suggests formation in a supra-subduction zone.

3. The poorly developed sheeted-dyke complex and well-developed plutonic sequence also indicates a tectonic setting with a slow spreading rate. The geochemical signature of the source region of the sheeted dykes is broadly MORB-like with a subduction input. The

ACCEPTED MANUSCRIPT

plagiogranites also have subduction-related signature are intimately associated with both the gabbros and the sheeted dykes indicating a co-genetic relationship.

4. The mafic dyke swarm crosscut both the ophiolite and the metamorphic sole rocks and have a less-marked subduction signature than, particularly, the sheeted dykes. This weaker subduction signature suggests that these melts may have passed through a slab window and that these dykes are not co-genetic with the gabbros and ultramafic rocks of the ophiolite.

5. The tholeiitic MORB-like basalts of the Bagh Complex represent Neo-Tethyan ocean floor, formed during the Cretaceous period after the breakup of Gondwana, whereas the associated OIB-like alkaline rocks are probably derived from a hotspot during Middle–Late Cretaceous. Most of the OIB-like and MORB-like lavas of the Bagh Complex possess negative Nb-Ta anomalies, consistent with continental crust contamination from fragments of crust that were incorporated into the Tethyan ocean basin during the breakup of Gondwana.

6. The Muslim Bagh Ophiolite has the geology of oceanic lithosphere but arc like geochemistry and so is more likely to formed in a supra-subduction zone environment, rather than a back-arc basin.

Acknowledgments

This work forms part of the PhD study of Mohammad Ishaq Kakar. We thank two anonymous reviewers for their constructive comments which improved the manuscript

ACCEPTED MANUSCRIPT

References

Ahmad, Z., Abbas, S.G., 1979. The Muslim Bagh ophiolite. In: Farah, A., DeJong, K.A. (Eds.), Geodynamics of Pakistan. Geological Survey of Pakistan, Quetta 243-250.

Aitchison, J.C., Ali, J.R., Davis, A.M., 2007. When and where did India and Asia collide? Journal of Geophysical Research: Solid Earth, 112, B05423, doi:10.1029/2006JB004706.

Ali, J.R., Aitchison, J.C., 2008. Gondwana to Asia: Plate tectonics, paleogeography and the biological connectivity of the Indian sub-continent from the Middle Jurassic through latest Eocene (166–35 Ma). Earth-Science Reviews 88(3), 145-166.

Ali, J.R., Aitchison, J.C., 2005. Greater India. Earth Science Reviews 72,169-188.

Allemann, F., 1979. Time of emplacement of the Zhob Valley ophiolite and Bela ophiolite, Balochistan (preliminary report). In: Farah, A., Dejong, K.A. (Eds.), Geodynamics of Pakistan: Quetta, Geological Survey of Pakistan 213- 242.

Arif, M., Jan, M.Q., 2006. Petrogenetic Significance of the chemistry of chromite in the Ultramafic-mafic Complexes of Pakistan. Journal of Asian Earth Sciences 27 (5), 1-19.

Asrarullah, Ahmad, Z. Abbas, S.G. 1979. Ophiolites in Pakistan: An introduction. In: A. Farah and K.A. DeJong (Eds.), Geodynamics of Pakistan. Geological Survey of Pakistan, Quetta, 181-192.

Baker, M.B., Beckett, J.R., 1999. The origin of abyssal peridotites; a reinterpretation of constraints based on primary bulk compositions. Earth and Planetary Science Letters 171, 49–61.

Beck, R., Burbank, W.D., Sercombe, W.J., Khan, A.M., Lawrence, R.D., 1996. Late Cretaceous ophiolite obduction and Paleocene India-Asia collision in the westernmost Himalaya. Geodynamica Acta 9, 114-144.

Beck, R.A., Burbank, D.W., Sercombe, W.J., Riley, G.W., Barndt, J.K., Berry, J.R., Afzal, J., Khan, M.A., Jurgen, H., Metje, J., Cheema, A., Shafique, N.A., Lawrence, R.D., Khan, M.A. 1995. Stratigraphic evidence for an early collision between northwest India and Asia. Nature 373, 55-58.

ACCEPTED MANUSCRIPT

Bedard, J.H., 1991. Cumulate recycling and crustal evolution in the Bay of Islands ophiolite. Journal of Geology, 99, 225–249.

Benn, K., Nicolas, A., Reuber, I., 1988. Mantle-crust transition zone and origin of wehrlitic magmas: evidence from the Oman Ophiolite. Tectonophysics, 151, 75–85.

Bernoulli, D., Weissert, H., Blome, C.D., 1990. Evolution of the Triassic Hawasina Basin, Central Oman Mountains. Geological Society, London, Special Publication 49, 189-202.

Boudier, F., Nicholas, A., 1995. Nature of the Moho transition zone in the Oman ophiolite. Journal of Petrology 36, 777–796.

Cai, K., Sun, M., Yuan, C., Zhao, G., Xiao, W., Long, X., Wu, F., 2010. Geochronological and geochemical study of mafic dykes from the northwest Chinese Altai: Implications for petrogenesis and tectonic evolution. Gondwana Research 18, 638–652.

Cannat, M., Karson, J.A., Miller, D.J., Agar, S.M., Barling, J., Casey, J.F., Ceuleneer, G. Dilek, Y., Fletcher, J., Fujibayashi, N. Gaggero, L., Gee, J.S., Hurst, S.D., Kelley, D.S., Kempton, P.D., Lawrence, M.R., Marchig, V., Mutter, C., Niida, K., Rodway, K., Ross, D.K., Stephens, C., Werner, C-D., Whitechurch, H., 1995. Proceedings of the ODP, Initial Reports, 153: College Station, TX.

Cannat, M., Sauter, D., Mendel, V., Ruellan, E., Okino, K., Escartin, J., Baala, M., 2006. Modes of seafloor generation at a melt-poor ultra-slow-spreading ridge. Geology, 34, 605-608.

Celik, O.F., 2007. Metamorphic sole rocks and their mafic dykes in the eastern Tauride belt ophiolites (southern Turkey): implications for OIB-type magma generation following slab break-off. Geological Magazine 144 (5), 849–866.

Chen, L., Ma, C.Q., Zhang, J.Y., Mason, R., Zhang, C.,, 2011. Mafic dykes derived from Early Cretaceous depleted mantle beneath the Dabie orogenic belt: implications for changing lithosphere mantle beneath eastern China. Geological Journal 46: 333–343.

Coleman, R.G., 1977. Ophiolite-Ancient oceanic lithosphere? Minerals and rocks. Springer-verlag, New York.

ACCEPTED MANUSCRIPT

Corfield, R.I., Searle, M.P., Pedersen, R.B., 2001. Tectonic setting, origin, and obduction history of the Spontang Ophiolite, Ladakh Himalaya, NW India. The Journal of Geology, 109(6), 715-736.

Davidson, J.P., Turner, S., Plank, T., 2013. Dy/Dy*: variations arising from mantle sources and petrogenetic processes. Journal of Petrology 54, 525-537.

Dick, H.J.B., Bullen, T., 1984. Chromium spinel as a petrogenetic indicator in abyssal and Alpine-type peridotites and spatially associated lavas. Contributions to Mineralogy Petrology 86, 54–76.

Dick, H.J.B., Fisher, R.L., 1984. Mineralogic studies of the residues of mantle melting abyssal and alpine-type peridotites. In: Kornprobst, J. (Ed.), Kimberlites II: The Mantle and Crust-Mantle Relationships, Amsterdam (Elsevier), 295-308.

Dilek, Y., Flower, M.F.J., 2003. Arc-trench rollback and forearc accretion: 2. A model template for ophiolites in Albania, Cyprus, and Oman. In: Dilek, Y., Robinson, P.T. (Eds.), Ophiolites in Earth History, Geological Society of London Special Publication 218, 43–68.

Dilek, Y., Thy, P., Hacker, B., Grundvig, S., 1999. Structure and petrology of Tauride ophiolites and mafic dyke intrusions (Turkey): implications for the Neotethyan Ocean. Geological Society of America 111, 1192–1216.

Elburg, M.A., Bons, P.D., Foden, J. Brugger, J., 2003. A newly defined Late Ordovician magmatic-thermal event in the Mt Painter Province, northern Flinders Ranges, South Australia. Australian Journal of Earth Sciences 50: 4, 611-631.

Elthon, D., Casey, J.F., Komor, S., 1982. Mineral chemistry of ultramafic cumulates from the north Arm Mountain massif of the Bay of island ophiolite: evidence for high pressure crystal fractionation of oceanic basalts. Journal of Geophysical Research, 87, 8717-8734.

Fitton, J.G., Saunders, A.D., Norry, M.J., Hardarson, B.S., Taylor, R.N., 1997. Thermal and chemical structure of the Iceland plume. Earth and Planetary Science Letters 153, 197–208.

Flower, F.J. Dilek, Y., 2003. Arc-trench rollback and forearc accretion: 1. A collision-induced mantle flow model for Tethyan ophiolites. In: Dilek Y. and Robinson P. T. (Eds.), Ophiolites in Earth History. Geological Society of London Special Publication 218, 21–41.

ACCEPTED MANUSCRIPT

Frey, F.A., Weis, D., Borisova, A.Y. Xu, G., 2002. Involvement of continental crust in the formation of the Cretaceous Kerguelen Plateau: New perspectives from ODP Leg 120 sites. Journal of Petrology 43, 1207-1239.

Gansser, A., 1964. Geology of the Himalayas. Wiley Interscience, London, 289p.

Gnos, E., Immenhauser, A., Peters, T.J., 1997. Late Cretaceous/Early Tertiary convergence between the Indian and Arabian plates recorded in ophiolites and related sediments Tectonophysics 271, 1-19.

Gnos, E., Khan, M., Mahmood, K., Khan, A.S., Naseer, A. Villa, I.M., 1998. Bela oceanic lithosphere assemblage and its relation to the Reunion hot spot. Terra Nova 10, 90-95.

Gopel, C., Allegre, C.J., Rong, H.X., 1984. Lead isotope study of the Xigaze ophiolite (Tibet): the problem of the relationship between magmatites (gabbros, dolerites, lavas) and tectonites (harzburgites). Earth and Planetary Science Letters 6, 301-310.

Green, O.R., Searle, M.P., Corfield, R.I., Corfield, R.M., 2008. Cretaceous-Tertiary carbonate platform evolution and the age of the India-Asia collision along the Ladakh Himalaya (Northwest India). The Journal of Geology, 116(4), 331-353.

Hastie, A.R., Kerr, A.C., Pearce, J.A., Mitchell, S.F., 2007. Classification of altered volcanic island arc rocks using immobile trace elements: Development of the Co-Th discrimination diagram. Journal of Petrology 48, 2341-2357.

Hastie, A.R., Mitchell, S.F., Treloar, P., Kerr, A.C., Neill, I., Barfod, D.N., 2013. Geochemical components in a Cretaceous island arc: The Th/La:$(Ce/Ce^*)_{Nd}$ diagram and implications for subduction initiation in the inter-American region. Lithos 162, 57-69.

Hofmann, C., Feraud, G., Courtillot, V., 2000. $^{40}Ar/^{39}Ar$ dating of mineral separates and whole rocks from the Western Ghats lava pile: further constraints on duration and age of the Deccan traps. Earth and Planetary Science Letters 180(1), 13-27.

Hooper, P., Widdowson, M., Kelley, S., 2010. Tectonic setting and timing of the final Deccan flood basalt eruptions. Geology 38, 839-842.

ACCEPTED MANUSCRIPT

HSC (Hunting Survey Corporation), 1960. Reconnaissance Geology of part of West Pakistan. A Colombo Plan cooperative project, Government of Canada, Toronto, 550.

Jaques, A.L., Green, D.H., 1980. Anhydrous melting of peridotite at 0-15 kb pressure and the genesis of tholeiitic basalts. Contributions to Mineralogy Petrology, 73, 287-310.

Kakar, M.I., 2011. Petrology, geochemistry and tectonic setting of the Muslim Bagh Ophiolite, Balochistan, Pakistan. PhD Thesis (unpublished), Centre of Excellence in Mineralogy, University of Balochistan, Quetta, 257p.

Kakar, M.I., Collins, A.S., Mahmood, K., Foden, J.D., Khan, M., 2012. U-Pb Zircon crystallization age of the Muslim Bagh Ophiolite: Enigmatic remains of an extensive pre-Himalayan arc. Geology, 40 (12), 1099-1102.

Kazmi, A.H., 1984. Petrology of the Bibai Volcanics, NE Balochistan. Geological Bulletin University of Peshawar 17, 43-51.

Kelemen, P.B., Shimizu, N., Salters, V.J.M., 1995. Extraction of mid-ocean-ridge basalt from the upwelling mantle by focused flow of melt in dunite channels. Nature, 375, 747–753.

Kelemen, P.B., Dick, H.J.B. Quick, J.E., 1992. Formation of harzburgite by pervasive melt/rock reaction in the upper mantle. Nature 358, 635-641.

Kerr, A.C., 2014. Oceanic plateaus. In: Holland, H.C. & Turekian K. (series eds). Treatise on Geochemistry 2nd Edition, Volume 4: Rudnick, R. (ed) Chapter 18, pp. 631-667. Elsevier.

Kerr, A.C., Khan, M., Mahoney, J.J., Nicholson, K. N., Hall, C.M., 2010. Late Cretaceous alkaline sills of the south Tethyan suture zone, Pakistan: Initial melts of the Réunion hotspot Lithos, 117, 161–171.

Khan, M., Kerr, A.C., Mahmood, K., 2007. Formation and tectonic evolution of the Cretaceous–Jurassic Muslim Bagh ophiolitic complex, Pakistan: Implications for the composite tectonic setting of ophiolites. Journal of Asian Earth Science 31, 112-127.

Khan, S-R., 2000. Petrology and geochemistry of a part of Waziristan Ophiolite, NW Pakistan. Unpublished PhD thesis, University of Peshawar, 253p.

ACCEPTED MANUSCRIPT

Khan, S-R., Jan, M. Q., Khan, T., and Khan, M. A. 2007. Petrology of the dykes from the Waziristan Ophiolite, NW Pakistan. Journal of Asian Earth Sciences, 29(2), 369-377.

Khan, S.D., Walker, D.J., Hall, S.A., Burke, K.C., Shah, M.T., Stockli, L., 2009. Did the Kohistan-Ladakh island arc collide first with India? Geological Society of America Bulletin 121, 366–384.

Koepke, J., Berndt, J., Feig, S.T., Holtz, F., 2007. The formation of SiO_2-rich melts within the deep oceanic crust by hydrous partial melting of gabbros. Contributions to Mineralogy and Petrology 153, 67-84.

Koepke, J., Feig, S.T., Snow, J., Freise, M., 2004. Petrogenesis of oceanic plagiogranites by partial melting of gabbros: An experimental study. Contributions to Mineralogy and Petrology 146, 414-432.

Kojima, S., Naka, T., Kimura, K., Mengal, J.M., Siddiqui, R.H., Bakht, M.S., 1994. Mesozoic radiolarians from the Bagh Complex in the Muslim Bagh area, Pakistan: their significance in reconstructing the geological history of ophiolites along the Neo-Tethys suture zone. Bulletin of Geological Survey Japan 45, 63–97.

Lytwyn, J.N., Casey, J.F., 1995. The geochemistry of post-kinematic mafic dike swarms and subophiolitic metabasites, Pozanti-Karsanti ophiolite, Turkey: evidence for ridge subduction. Geological Society of American Bulletin 107, 830–850.

Mahmood, K., Boudier, F., Gnos, E., Monié, P., Nicolas, A., 1995. $^{40}Ar/^{39}Ar$ dating of the emplacement of the Muslim Bagh ophiolite, Pakistan. Tectonophysics 250, 169-181.

Mahoney, J.J., Duncan, R.A., Khan, W., Gnos, E., McCormick, G.R., 2002. Cretaceous volcanic rocks of the south Tethyan suture zone, Pakistan: implications for the Réunion hotspot and Deccan Traps. Earth and Planetary Science Letters 203, 295–310.

Mahoney, J.J., Frei, R., Tejada, M.L.G., Mo, X.X., Leat, P.T. Nagler, T.F., 1998. Tracing the Indian Ocean mantle domain through time: Isotopic results from Old West Indian, East Tethyan, and South Pacific seafloor. Journal Petrology 39(7), 1285-1306.

ACCEPTED MANUSCRIPT

Malpas, J., 1978. Magma generation in upper mantle, field evidence from ophiolite suites, and application to generation of oceanic lithosphere. Philosophical Transactions of the Royal Society London Series A, 288, 527–545.

Malpas, J., Zhou, M.-F., Robinson, P.T. Reynolds, P., 2003.Geochemical and geochronological constraints on the origin and emplacement of the Yarlung–Zangbo ophiolites, Southern Tibet. In: Dilek, Y. & Robinson, P. T. (Eds.), Ophiolites through Earth History. Geological Society, London, Special Publication 218, 191–206.

Manan, R.A., 2013. Triassic–Jurassic rocks of the western Suleiman fold belt, Balochistan, Pakistan. PhD Thesis (unpublished), Centre of Excellence in Mineralogy, University of Balochistan, Quetta, 173p.

Mengal, J.M., Kimura, K., Siddiqui, M.R.H., Kojima, S., Naka, T., Bakht, M.S., Kamada, K., 1994. The lithology and structure of a Mesozoic Sedimentary-igneous assemblage beneath the Muslim Bagh ophiolite, Northern Balochistan, Pakistan, Bulletin of Geological Survey of Japan, 45, 51-61.

Michael, P.J., Langmuir, C.H., Dick, H.J.B., Snow, J.E., Goldstein, S.L., Graham, D.W., Edmonds, H.N., 2003. Magmatic and amagmatic seafloor generation at the ultraslow-spreading Gakkel ridge, Arctic Ocean. Nature, 423(6943), 956-961.

Muller, R.D., Gaina, C., Clarke, S., 2000. Seafloor spreading around Australia. In: Veevers, J.J. (Ed.), Billion-Year Earth History of Australia and Neighbours in Gondwanaland. GEMOC Press, Sydney 18–28.

Mysen, B.O., Kushiro, I., 1977. Compositional variation of coexisting phases with degree of melting of peridotite in the upper mantle. American Mineralogist, 62, 843–865.

Najman, Y., Appel, E., Boudagher-Fadel, M., Bown, P., Carter, A., Garzanti, E., Vezzoli, G., 2010. Timing of India-Asia collision: Geological, biostratigraphic, and palaeomagnetic constraints. Journal of Geophysical Research: Solid Earth 115, B12416, doi: 10.1029/2010JB007673.

ACCEPTED MANUSCRIPT

Naka, T., Kimura, K., Mengal, J.M., Siddiqui, R.H., Kojima, S., Sawada, Y., 1996. Mesozoic sedimentary-igneous Complex, Bagh Complex, in the Muslim Bagh Area, Pakistan. Opening and Closing Ages of the Ceno-Tetheyan Branch. In: Yajima, J., Siddiqui, R.H. (Eds.), Proceedings of Geoscience Colloquium, Geoscience Laboratory, Geological Survey of Pakistan, Islamabad 16, 47-94.

Nicolas, A., 1989. Structures of Ophiolites and Dynamics of Oceanic Lithosphere. Kluwer, Dordrecht, 367p.

Nicolas, A., Boudier, F., Meshi, A., 1999. Slow spreading accretion and mantle denudation in the Mirdita ophiolite (Albania). Journal of Geophysical Research: Solid Earth 104(B7), 15155-15167.

Nicolas, A., Prinzhofer, A. 1983. Cumulative or residual origin for the transition zone in ophiolites: structural evidence. Journal of Petrology, 23, 188-206.

Ohara, Y., Stern, R.J., Ishii, T., Yurimoto, H.T., Yamazaki, T., 2002. Peridotites from the Mariana Trough: first look at the mantle beneath an active back-arc basin. Contributions to Mineralogy Petrology 143, 1–18.

Otsuki, K., Hoshino, K., Anwar, M., Mengal, J.M., Broahi, I.A., Fatmi, A.N., Yuji, O., 1989. Breakup of Gondwanaland and emplacement of ophiolitic complexes in Muslim Bagh area of Balochistan, Pakistan. Mineral Development of Pakistan Hiroshima University, 33–57.

Payne, J.L., Barovich, K.M., Hand, M., 2006. Provenance of metasedimentary rocks in the northern Gawler Craton, Australia: implications for Palaeoproterozoic reconstructions. Precambrian Research 148, 275-291.

Pearce J.A., 1996. A users guide to basalt discrimination diagrams. In Trace Element Geochemistry of Volcanic Rocks: Applications for Massive Sulphide Exploration, vol. 12 (ed. Wyman, D.A). Geological Association of Canada Short Course Notes, pp. 79-113.

Pearce, J.A., 1982. Trace element characteristics of lavas from destructive plate margins. In: Thorpe, R.S., (ed.), Andesites: Orogenic andesites and related rocks, Wiley. 525-548.

ACCEPTED MANUSCRIPT

Pearce, J.A., Peate, D.W., 1995. Tectonic implications of the composition of volcanic arc magmas. Annual Review of Earth and Planetary Sciences 23, 251-285.

Plummer, P.S., 1996. The Amirante ridge/ trough complex: response to rotational Transform rift/ drift between Seychelles and Madagascar. Terra. Nova 8, 34-47.

Plummer, P.S., Belle, E.R., 1995. Mesozoic tectono-stratigraphic evolution of the Seychelles micro-continent. Sedimentary Geology 96, 73-91.

Polat, A., Casey J.F. 1995. A structural record of the emplacement of the Pozanti-Karsanti ophiolite onto the Menderes-Taurus block in the late Cretaceous, eastern Taurides, Turkey. Journal of Structural Geology 17(12), 1673-1688.

Polat, A., Casey J.F., Kerrich, R. 1996. Geochemical characteristics of accreted material beneath the Pozanti-Karsanti ophiolite, Turkey: Intra-oceanic detachment, assembly and obduction." Tectonophysics 263, 249-276.

Powell, C.M., Roots, S.R., Veevers, J.J., 1988. Pre-breakup continental extension in East Gondwanaland and the early opening of the eastern Indian Ocean. Tectonophysics 155, 261–283.

Qayyum, M., Lawrence, R.D., Niem, A.R. 1997. Discovery of the palaeo-Indus delta-fan complex. Journal of the Geological Society, London 154, 753–756.

Qayyum, M., Niem, A.R., Lawrence, R.D., 1996. Newly discovered Paleogene deltaic sequence in Katawaz basin, Pakistan and its tectonic implications. Geology 24, 835-838.

Robertson, A.H.F., 2002. Overview of the genesis and emplacement of Mesozoic ophiolites in the Eastern Mediterranean Tethyan region. Lithos 65, 1– 67.

Robertson, A.H.F., Searle, M.P., 1990. The Northern Oman Tethyan continental margin: stratigraphy, structure, concepts and controversies. In: A.H.F. Robertson, M. P., Searle and A.C. Ries (Eds.), The Geology and Tectonics of the Oman Region. Geological Society of London Special Publication 49, 3-25.

Robinson, P.T., Malpas, J., Dilek, Y., Zhou, M-F., 2008. The significance of sheeted dike complexes in ophiolites. Geological Society of America, Geology Today 18 (11), 4-10.

ACCEPTED MANUSCRIPT

Salam, A. and Ahmed, Z. 1986. Ophiolitic Ultramafic-mafic rocks from Bagh area. Acta Mineralogica Pakistanica 2, 65-73.

Sawada, Y., Nageo, K., Siddiqui, R.H., Khan, S.R., 1995. K-Ar ages of the Mesozoic Igneous and metamorphic rocks from the Muslim Bagh area, Pakistan. Proceedings of Geoscience Colloquium Geoscience Laboratory, Geological Survey of Pakistan 12, 73-90.

Sawada, Y., Siddiqui, R.H., Khan, S.R., Aziz, A., 1992. Mesozoic igneous activity in the Muslim Bagh area, Pakistan, with special reference to hotspot magmatism related to the break-up of the Gondwanaland: Proceedings of Geoscience Colloquium Geoscience Laboratory, Geological Survey of Pakistan 1, 21–70.

Searle, M., Corfield, R. I., Stephenson, B., McCarron, J., 1997. Structure of the north Indian continental margin in the Ladakh-Zanskar Himalayas: implications for the timing of obduction of the Spontang ophiolite, India-Asia collision and deformation events in the Himalaya. Geological Magazine 134 (3), 297-316.

Sengor, A.M., 1987. Tectonics of the Tethysides; orogenic collage development in a collisional setting. Annual Review of Earth and Planetary Sciences 15, 213-244.

Shervais, J.W., 2001. Birth, death, and resurrection; the life cycle of suprasubduction zone ophiolites. Geochemistry, Geophysics, Geosystems 2, 45, 2000GC000080.

Siddiqui, R.H., Aziz, A., Mengal, J. M., Hoshino, K., Sawada, Y., 1996. Geology, petrochemistry and tectonic evolution of Muslim Bagh Ophiolite Complex Balochistan. Pakistan Geologica, Geoscience Laboratory, Geological Survey Pakistan, Islamabad 3, 11-46.

Siddiqui R H, Mengal J M, Hoshino K, Sawada Y, Brohi I A (2011). Back-Arc basin signatures represented by the sheeted dykes from the Muslim Bagh Ophiolite Complex, Balochistan, Pakistan. Sindh University Research Journal 43: 51–62.

Suhr, G., Hellebrand, E., Snow, J.E., Seck, H.A., Hofmann, A.W., 2003. Significance of large, refractory dunite bodies in the upper mantle of the Bay of Islands Ophiolite. Geochemistry Geophysics Geosystems 4, Article No. 8605.

ACCEPTED MANUSCRIPT

Sun, S.-s., McDonough, W.F., 1989. Chemical and isotope systematics of oceanic basalts: implications for mantle composition and processes. Magmatism in the Ocean Basins. Geological Society of London, Special Publication 42, 313–345.

Van Vloten, R., 1967. Geology and chromite deposits of the Nisai area, Hindu Bagh mining district, West Pakistan. Geological Survey of Pakistan 2, 32p.

Varga, R.J. 2003, the sheeted dike complex of the Troodos ophiolite and its role in understanding mid-ocean ridge processes: In: Dilek, Y., and Newcomb, S., (Eds.), Ophiolite Concept and the Evolution of Geologic Thought: Geological Society of America Special Paper 373, 323-335.

Winchester, J.A., Floyd, P.A., 1976. Geochemical magma type discrimination: application to altered and metamorphosed basic igneous rocks. Earth and Planetary Science Letters 28, 459–469.

Xiao, B., Yu, H., Chen, G., Qi, L., Zhao, T.P., Zhou, M.-F., 2003. Geochemistry and tectonic environment of the Dazhuka ophiolite in the Yarlung-Zangbo suture zone, Tibet. Geochemistry Journal 37, 311–324.

Xiao, X.C. 1984., The Xigaze ophiolite in southern Tibet and related geotectonic problems. In: Li, G.C. (Ed.), Achievements in Sino-French Himalaya Investigations. Geological Publishers House, Beijing 143–162.

Xiong, Y., Khan, S D., Mahmood, K., Sisson, V.B., 2011. Lithological mapping of Bela ophiolite with remote-sensing data. International Journal of Remote Sensing, 32(16), 4641-4658.

Xu, Y-G., Lan, J-B., Yang, Q-J., Huang, X-L., Qiu, H-N., 2008. Eocene break-off of the Neo-Tethyan slab as inferred from intraplate-type mafic dykes in the Gaoligong orogenic belt, eastern Tibet, Chemical Geology 255, 439–453.

Zhou, M-F., Robinson, P.T., Malpas, J., Edwards, S.J., Qi, L., 2005. REE and PGE geochemical constraints on the formation of dunites in the Luobusa ophiolite, Southern Tibet. Journal of Petrology 46, 615–639.

ACCEPTED MANUSCRIPT

Zhou, M-F., Robinson, P.T., Malpas, J., Li, Z., 1996. Podiform chromitites in the Luobusa ophiolite (Southern Tibet): implications for mantle-melt interaction and chromite segregation. Journal of Petrology, 37, 3–21.

Zhu, B., Kidd, W. S., Rowley, D. B., Currie, B. S., Shafique, N., 2005. Age of initiation of the India-Asia collision in the east-central Himalaya. Journal of Geology, 113(3), 265-285.

ACCEPTED MANUSCRIPT

ACCEPTED MANUSCRIPT

Figure Captions

Figure 1: Geological Map of the Muslim Bagh area showing the Muslim Bagh Ophiolite, Bagh Complex, the Flysch Zone and the Indian passive margin sediments, (after Hunting Survey Corporation (1960), Van Vloten (1967), Siddiqui et al. (1996) and this study.

Figure 2: Schematic log of the Muslim Bagh Ophiolite showing the ophiolite suite and the attached metamorphic sole rocks. Not to scale. The inset is log of the cumulate sequence of the crustal rocks from the Muslim Bagh Ophiolite (after Salam and Ahmed, 1986).

Figure 3 a-d: Paleo-tectonic reconstruction of Muslim Bagh Ophiolite and Bagh Complex from Early Cretaceous to present 145-0Ma. Based on published work, see the text for detail. Key: Bs=Bagh Sedimentary unit, Bbc=Bagh basalt-chert unit, Bhm=Bagh hyaloclastite-mudstone unit, M=Marion, R=Reunion hotspot, NER= Ninety East Ridge.

Figure 4: a) Layered gabbros from the plutonic section of crustal rocks; b) Photomicrograph of gabbro showing subhedral to anhedral plagioclase (Pl), subpoikilitic clinopyroxene (Cpx) containing minor olivine (Ol) (crossed polars x 55); c) Sheeted dykes showing a trend from upper right to lower left corner; d) Amphibolite after dolerite showing altered plagioclase (Alt Pl) and secondary amphibole (Amp) (plane polarized light x10); e) Plagiogranite inclusions in dolerites of the sheeted dyke complex; f) Interlocking grains of plagioclase (Pl) and quartz (Qz) in plagiogranite, small grains of zircon can also seen (crossed polars x10).

Figure 5: Variation diagrams of representative major and trace elements against MgO, for the different rock types of the Muslim Bagh Ophiolite and the Bagh Complex.

Figure 6: (a) Co-Th classification plot (Hastie et al., 2007); (b) Nb/Y vs. Zr/Ti classification plot (Pearce, 1996); (c) plot of $(^{87}Sr/^{86}Sr)_i$ vs. $\varepsilon(Nd)_i$ (where i = 80 Ma for the Muslim Bagh

ACCEPTED MANUSCRIPT

Ophiolite rocks and 100 Ma for the Bagh Complex rocks). Indian Ocean MORB field at 80 Ma from Mahoney et al. (1998); Kerguelen data sources listed in Kerr (2014).

Figure 7: Chondrite-normalised (Sun and McDonough, 1989) REE plots for the Muslim Bagh Ophiolite and the Bagh Complex.

Figure 8: N-MORB-normalised (Sun and McDonough, 1989) multi-element diagrams for the Muslim Bagh Ophiolite and the Bagh Complex.

Figure 9: Plots of (a) Zr/Y vs. Nb/Y. Icelandic plume array from Fitton et al. (1997). Indian Ocean MORB (Central Indian Ridge and Southwest Indian Ridge) and East Pacific Rise (EPR) fields compiled from compiled data available on the PETDB website (http://www.earthchem.org/petdb - accessed 25/7/2013); (b) Nb/Yb vs. Th/Yb after Pearce and Peate (1995); (c) Dy/Yb vs. Dy/Dy* [after Davidson et al. (2013) – Dy/Dy* defined as: $Dy_N/(La_N^{4/13}*Yb_N^{9/13})$ (where N denotes chondrite normalised values) and is a measure of the 'concavity' of a REE pattern]. MORB/OIB fields and the amphibole trend are also from Davidson et al. (2013). (d) $(Ce/Ce^*)_{Nd}$ vs. Th/La [after Hastie et al. (2013) $(Ce/Ce^*)_{Nd}$ defined as: $Ce_N/(La_N^{2/3}\times Nd_N^{1/3})$ (where N denotes chondrite normalised values) Detritus fields, GLOSS II and N-MORB are also from Hastie et al. (2013).

Figure 10: Schematic cross sections showing the proposed tectonic evolution of the Muslim Bagh Ophiolite Complex. See text for more details. A) Separation of India from Afro-Arabia and Australia-Antarctica, B) Emplacement of Bbc and Bhm units, C) Short lived subduction, D) slab roll-back due to splitting of the nascent arc and the formation of the Muslim Bagh Ophiolite crust, E) The formation of the metamorphic sole and initial intra-oceanic detachment/obduction of ophiolite followed by the emplacement of mafic dyke swarm into both the metamorphic sole and the mantle section of the ophiolite through a

ACCEPTED MANUSCRIPT

slab window, F) The juxtaposition and emplacement of the Muslim Bagh Ophiolite along with underlying Bagh Complex onto the Indian continental margin, G) The present-day Muslim Bagh Ophiolite.

Tables

Table 1 - Representative major oxides, trace elements and Sr-Nd isotopes of the Muslim Bagh Ophiolite and the Bagh Complex.

Online Appendix 1 - Sample number, rock type, co-ordinates, field features, lithology and mineralogical and textural features.

Online Appendix 2 - International reference materials JB-1A, NIM-G and BIR-1 repeatedly analysed during the course of the study.

Online Appendix 3 - Full data set of major oxides (wt.%) trace elements (ppm) and Sr-Nd isotopes of Muslim Bagh Ophiolite mafic rocks and the volcanic rocks of Bagh Complex.

ACCEPTED MANUSCRIPT

ACCEPTED MANUSCRIPT

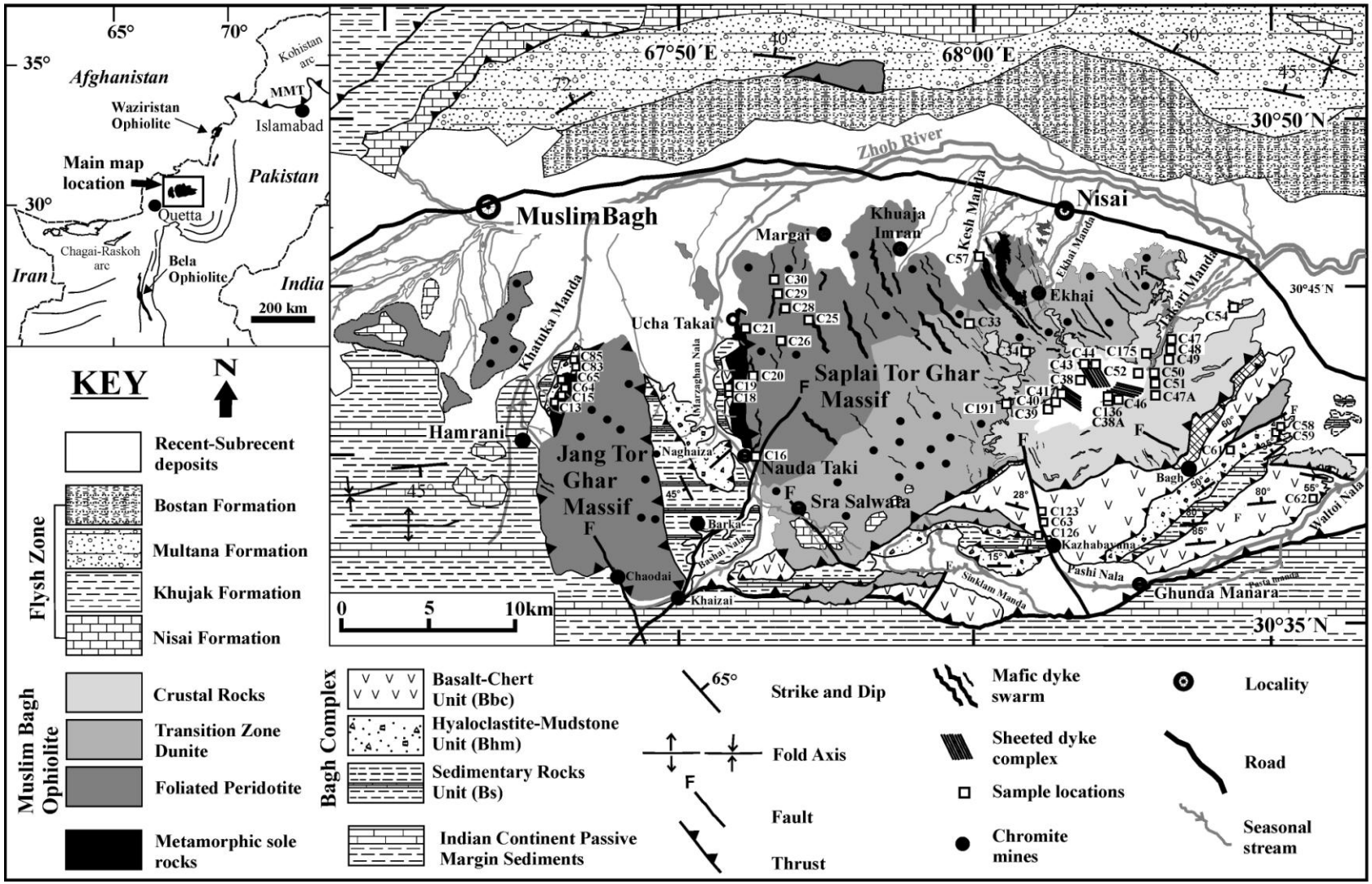

ACCEPTED MANUSCRIPT

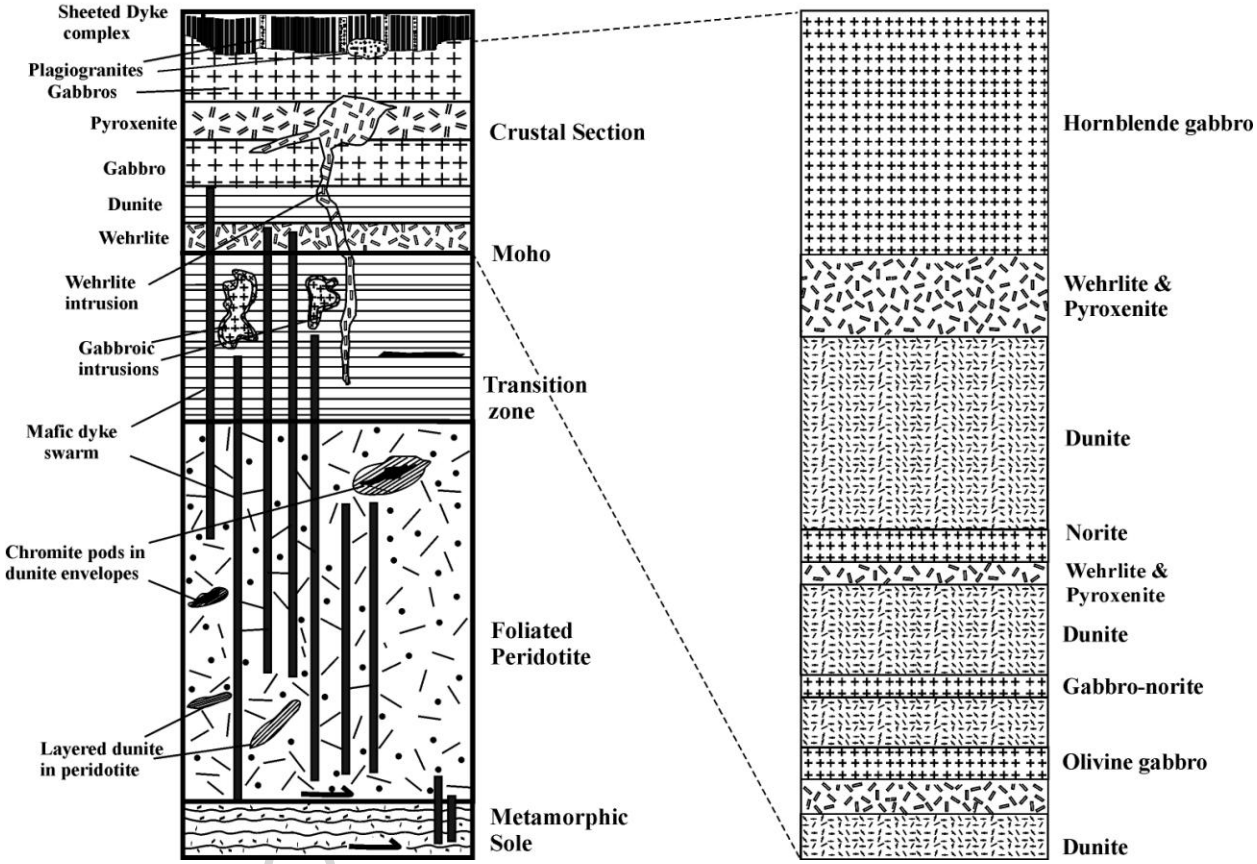

ACCEPTED MANUSCRIPT

Kakar et al Muslim Bagh Ophiolite Figure 3

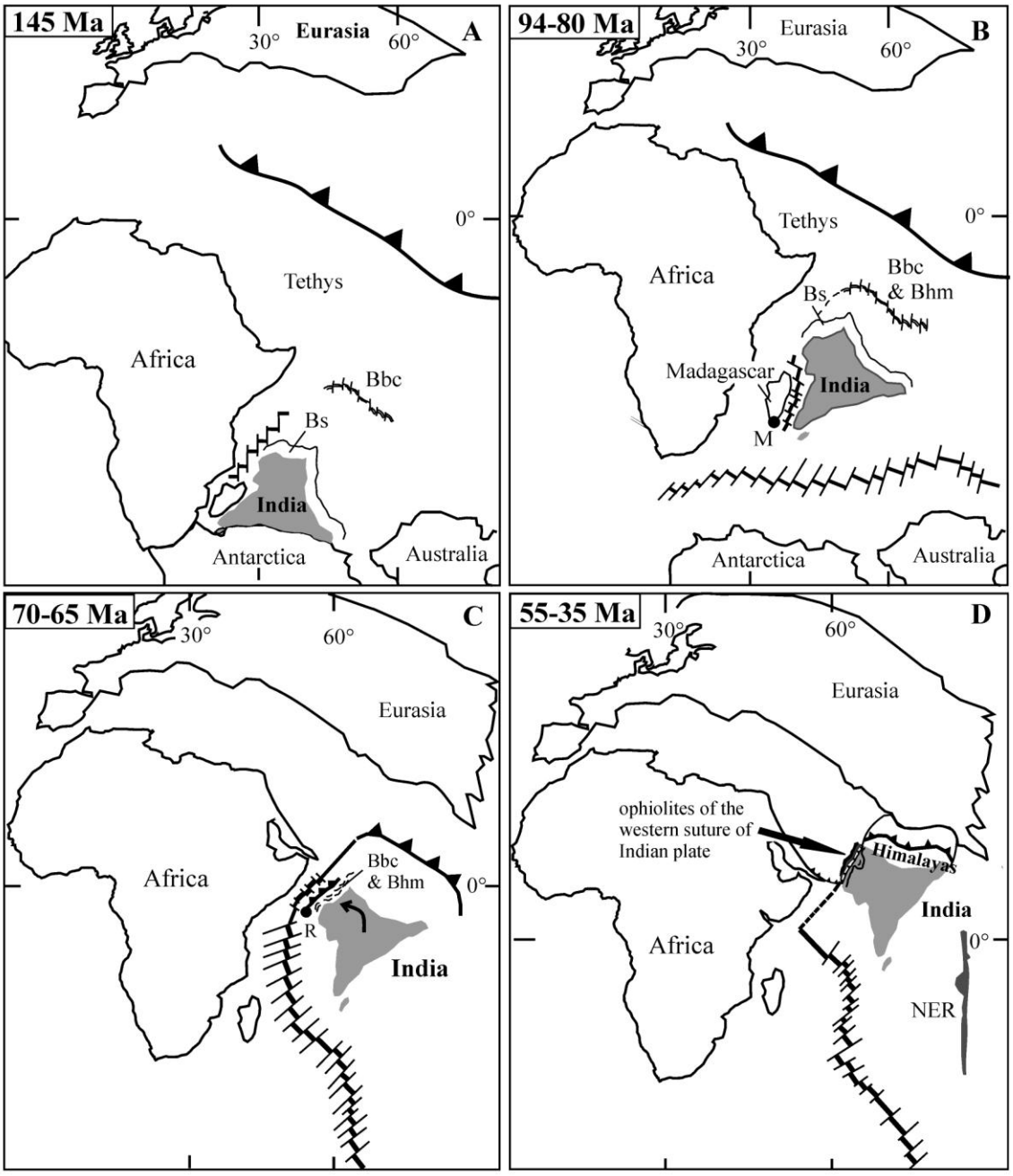

ACCEPTED MANUSCRIPT

Kakar et al. Muslim Bagh Ophiolite Figure 4

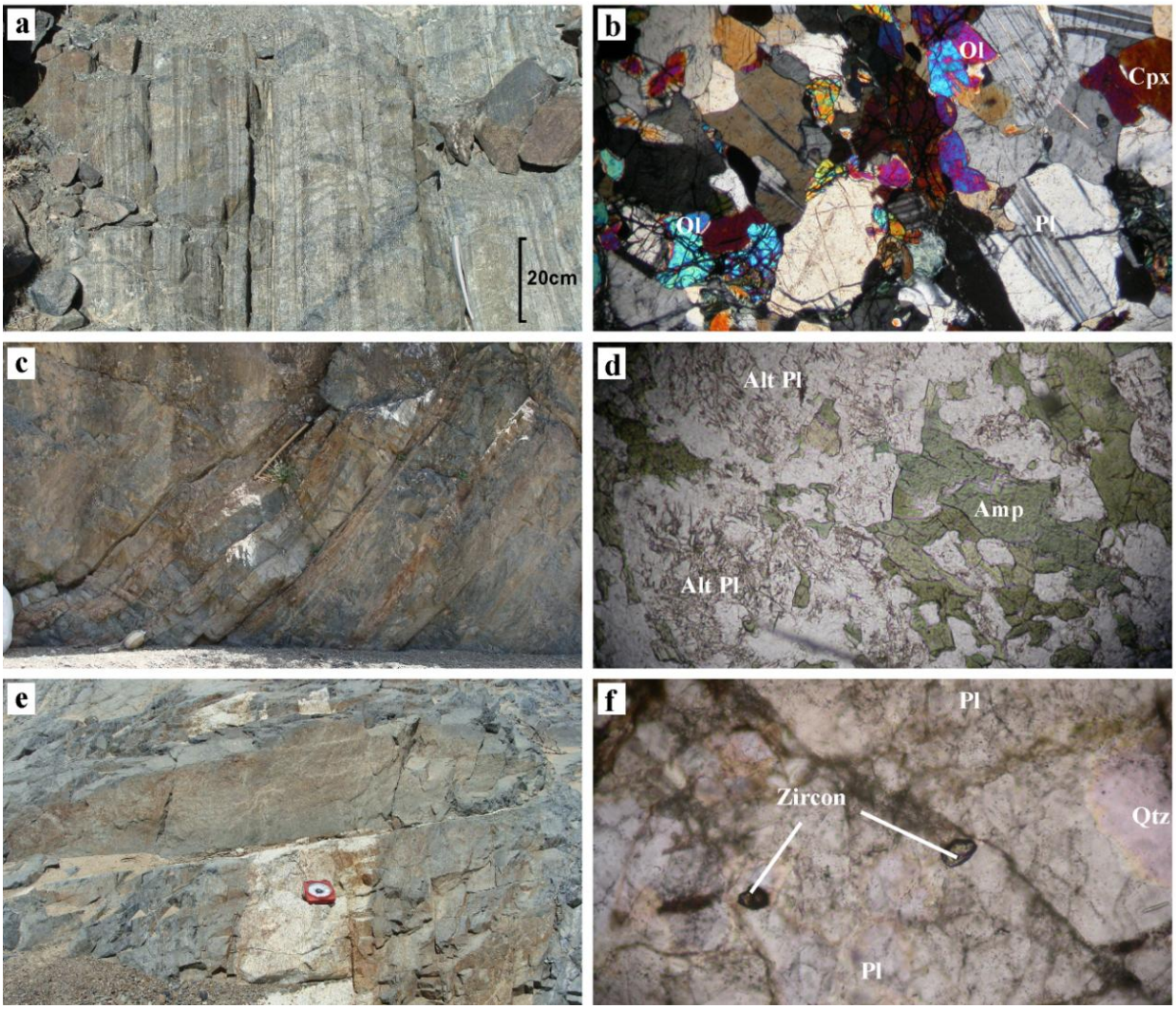

ACCEPTED MANUSCRIPT

Kakar et al Muslim Bagh Ophiolite Figure 5

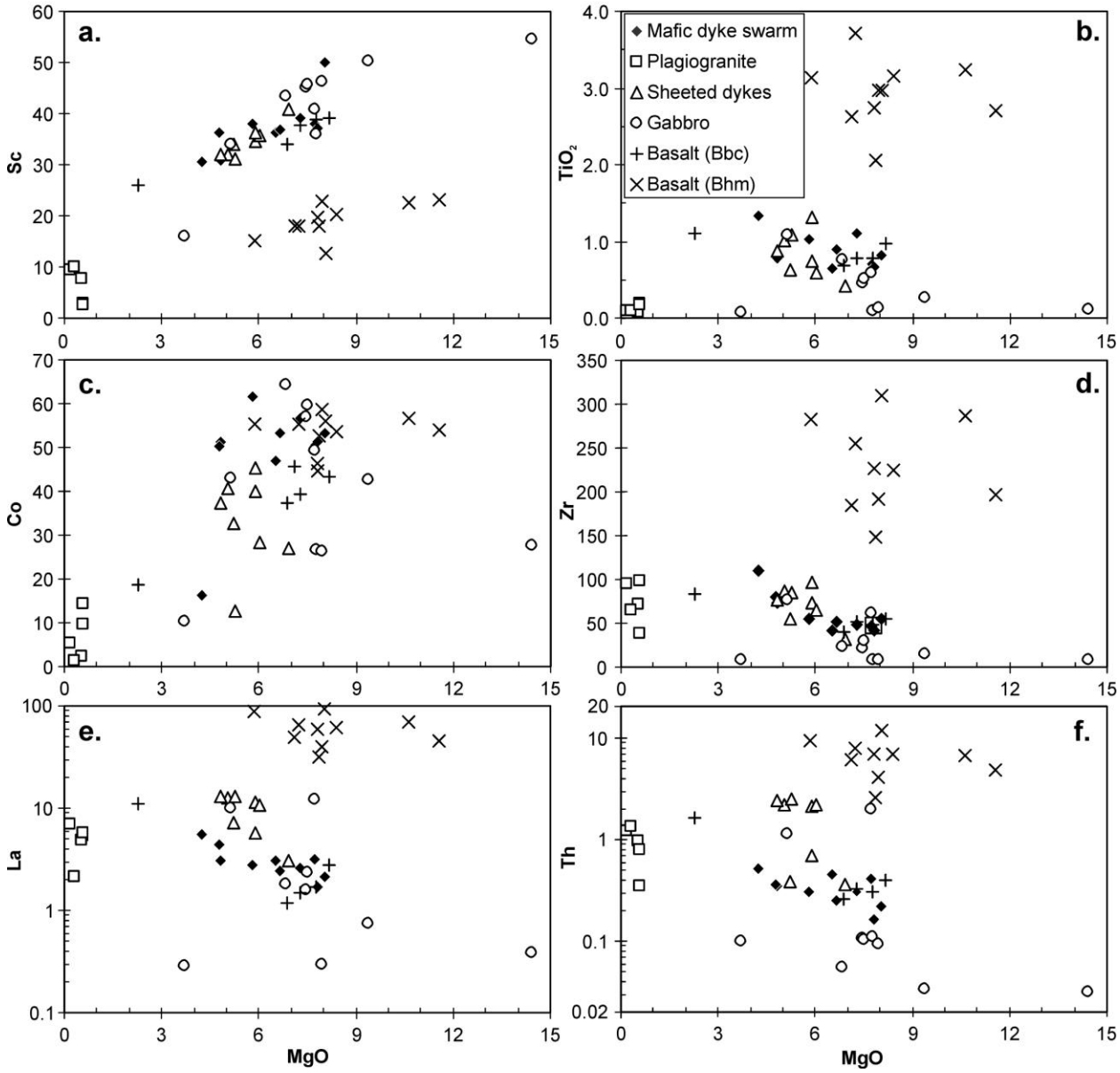

ACCEPTED MANUSCRIPT

Kakar et al Muslim Bagh Ophiolite Figure 6

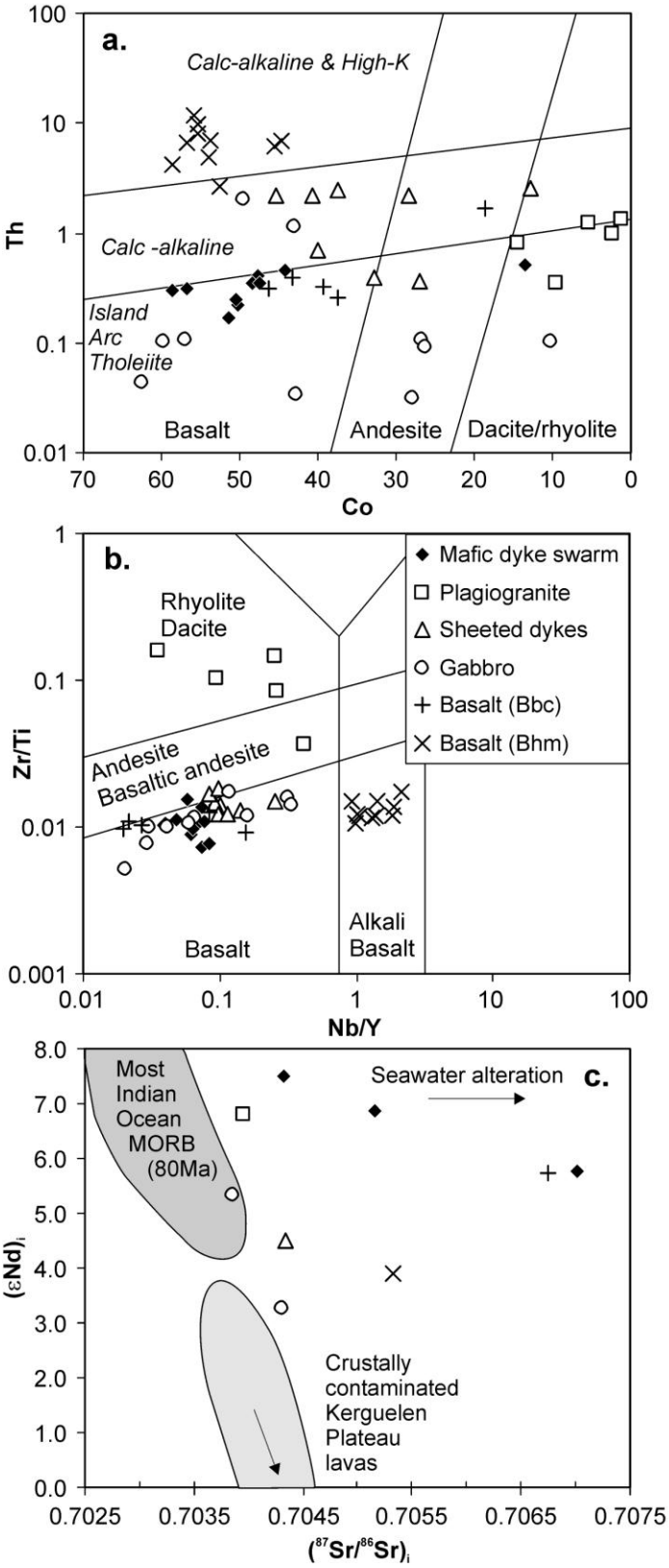

ACCEPTED MANUSCRIPT

Kakar et al. Muslim Bagh Ophiolite Figure 7

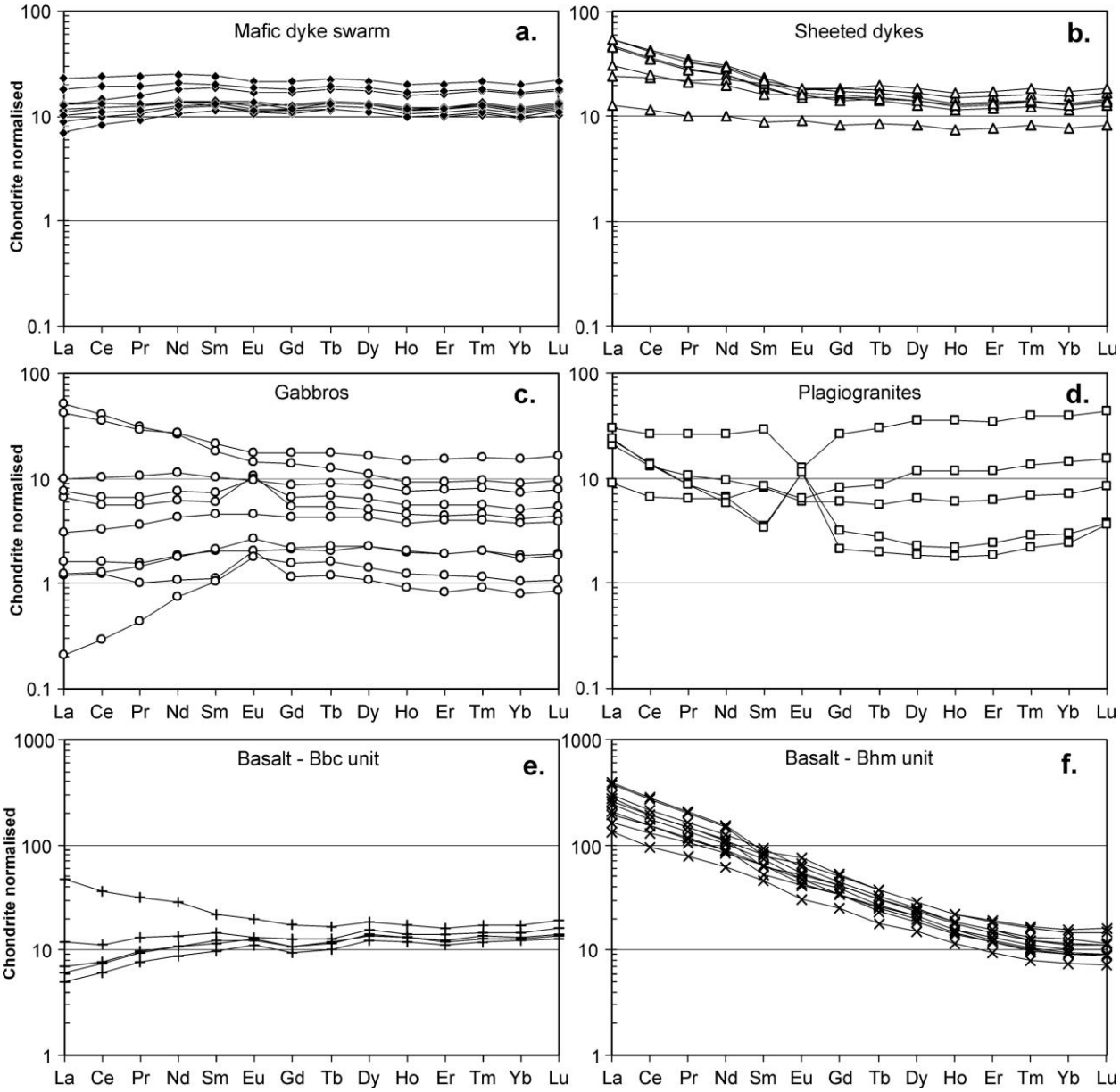

ACCEPTED MANUSCRIPT

Kakar et al. Muslim Bagh Ophiolite Figure 8

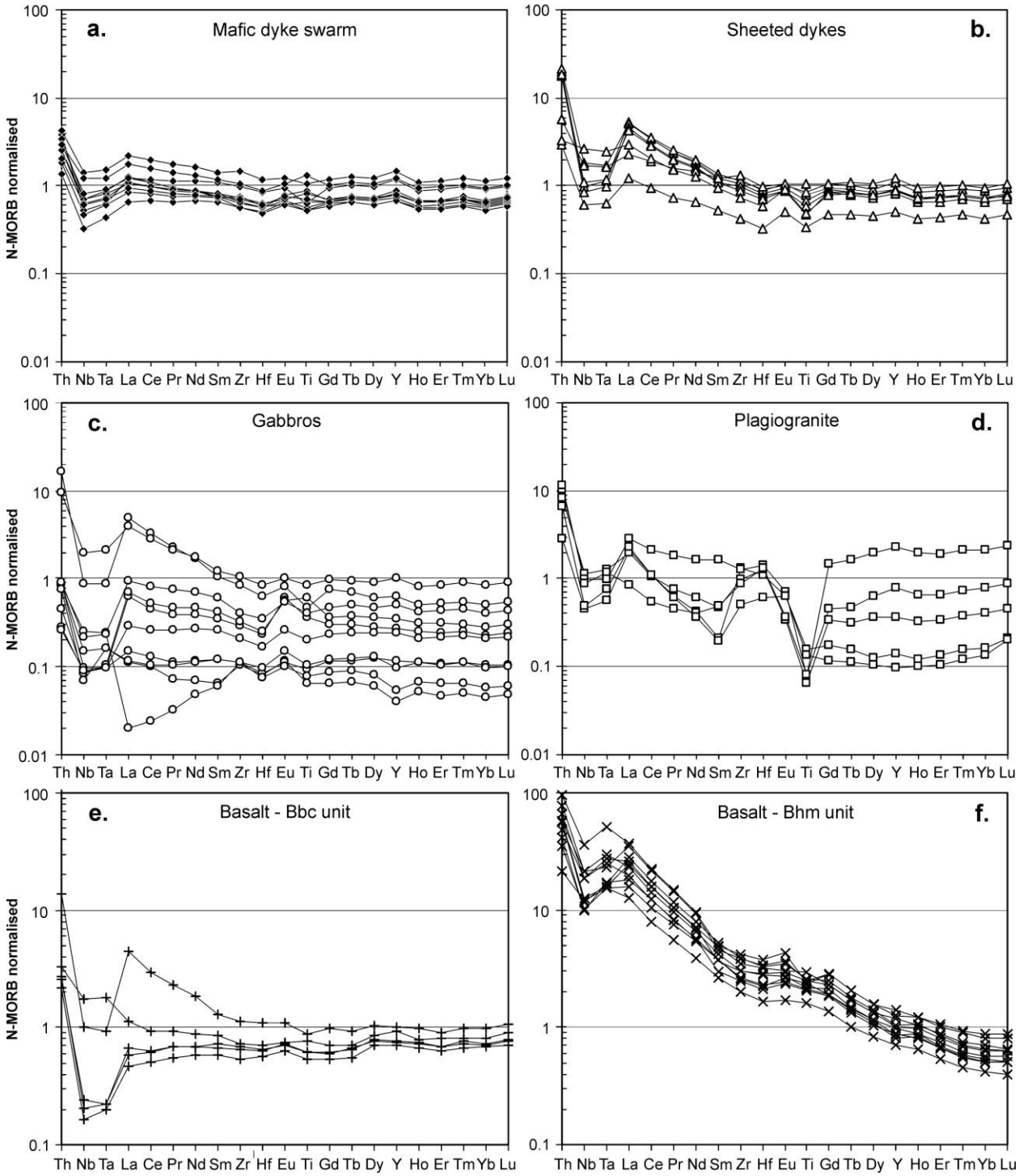

ACCEPTED MANUSCRIPT

Kakar et al Muslim Bagh Ophiolite Figure 9

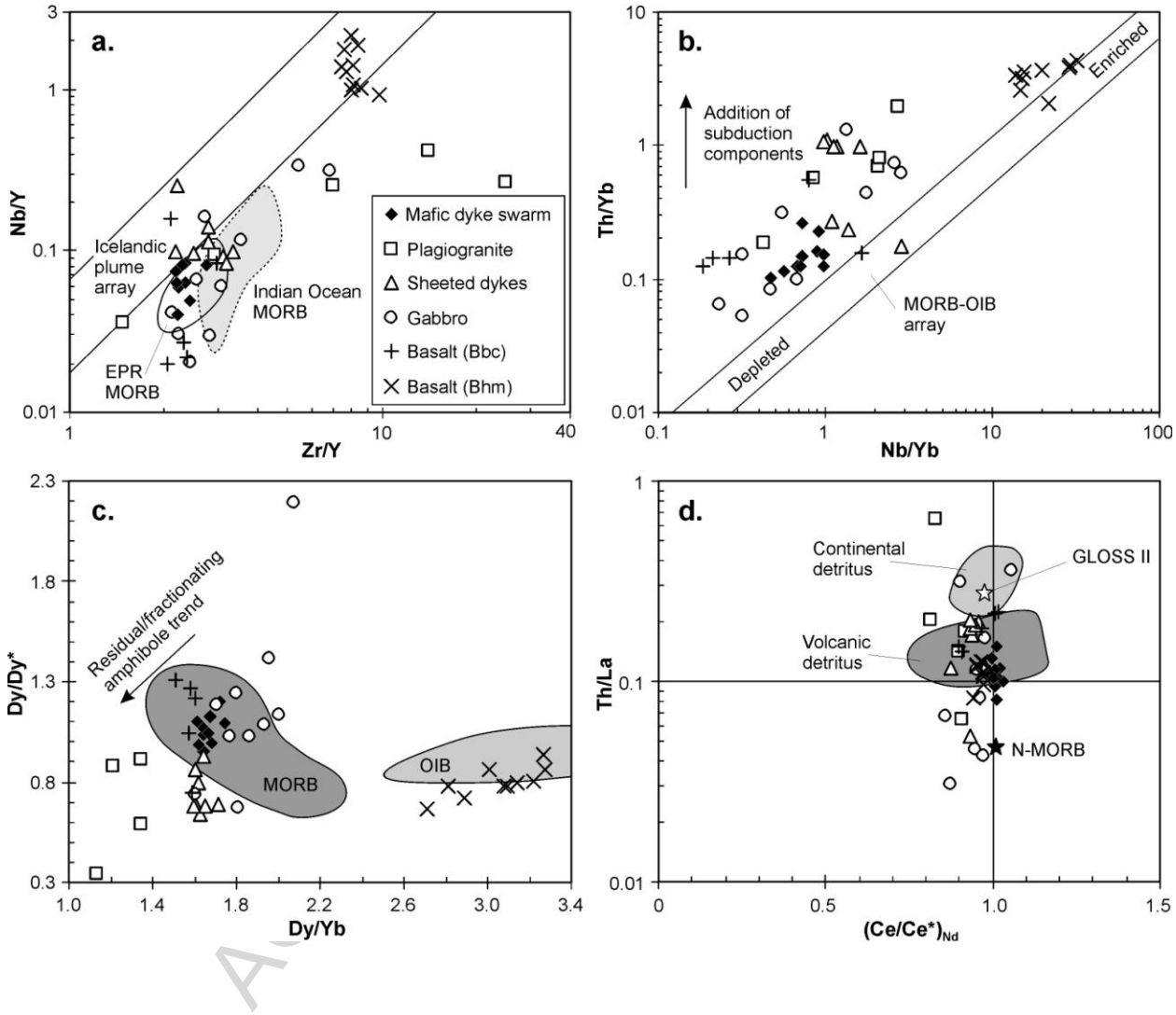

ACCEPTED MANUSCRIPT

Kakar et al Muslim Bagh Ophiolite Figure 10

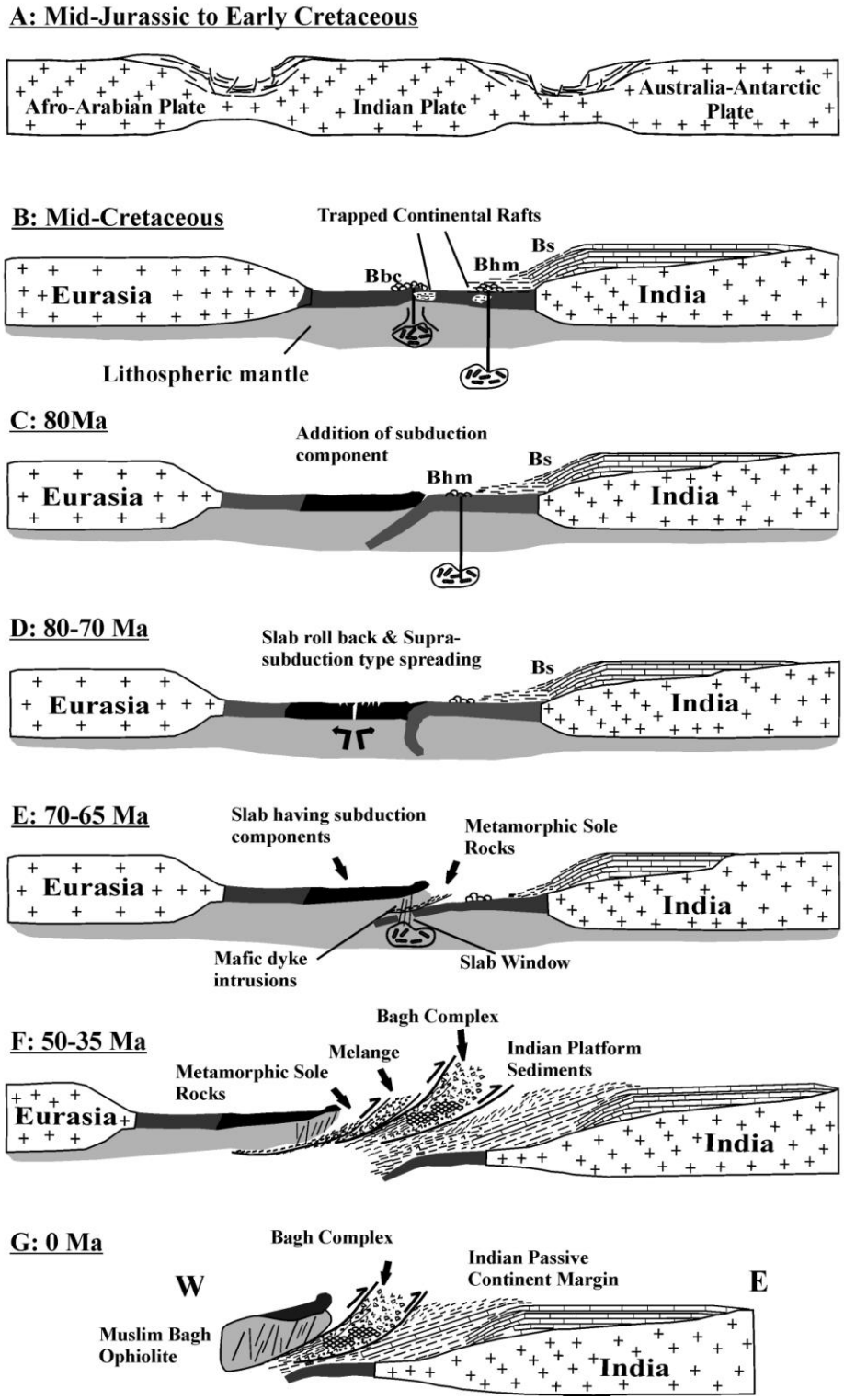

ACCEPTED MANUSCRIPT

Table 1. Representative major oxides, trace elements and Sr-Nd isotopes of the Muslim Bagh ophiolite and the Bagh complex

Rock	Mds	Mds	Mds	Plag Gr	Plag Gr	Sd	Sd	Sd	Gabbro
Sample	**C16**	**C28**	**C29**	**C136**	**C37A**	**C39**	**C40**	**C43**	**C34**
SiO_2 (wt.%)	51.21	49.05	50.34	74.61	78.50	54.15	54.22	49.17	50.22
TiO_2	0.66	0.82	1.03	0.20	0.08	0.87	1.09	0.42	1.09
Al_2O_3	15.09	14.73	15.00	12.47	11.95	15.17	15.06	18.75	14.66
Fe_2O_3	9.51	9.44	11.92	2.97	0.91	11.68	12.66	9.05	11.77
MnO	0.16	0.16	0.22	0.04	0.01	0.22	0.06	0.27	0.22
MgO	6.50	8.03	5.80	0.57	0.52	4.83	5.26	6.92	5.15
CaO	9.91	12.49	8.30	4.52	3.63	8.63	8.91	12.88	9.93
Na_2O	3.85	2.90	4.45	2.95	3.35	3.22	1.07	2.05	4.33
K_2O	1.09	0.17	0.57	0.18	0.38	0.44	0.22	0.38	0.65
P_2O_5	0.08	0.06	0.08	0.03	0.01	0.19	0.18	0.04	0.13
LOI	2.44	2.74	2.45	0.55	1.02	1.06	2.04	0.95	1.97
Total	100.50	100.59	100.17	99.09	100.38	100.46	100.76	100.88	100.12
Sc (ppm)	36.2	50.1	37.9	2.8	7.7	32.0	31.2	40.9	34.0
V	281	290	413	52	20	303	326	207	409
Cr	97	220	49	30	4	30	5	56	21
Co	44.2	50.2	58.6	9.6	2.2	37.3	12.7	27.0	43.0
Ni	66	107	80	99	3	12	13	43	23
Cu	76.6	118.7	165.8	34.1	8.5	105.8	13.9	18.7	90.7
Zn	67.2	68.8	114.6	23.4	12.6	89.1	20.4	69.5	90.6
Ga	12.2	11.7	14.4	10.4	9.6	15.0	16.0	13.3	12.6
Rb	26.4	3.3	11.7	1.8	4.5	3.7	2.5	5.2	7.6
Sr	142	338	178	211	194	296	287	153	355
Y	19.3	22.9	24.3	3.9	10.3	24.8	30.4	14.4	28.6
Zr	42	56	54	98	72	77	84	31	77
Nb	1.23	1.10	1.48	1.04	2.61	2.25	4.25	1.42	4.58
Sn	0.79	0.93	1.24	1.08	0.46	0.96	1.04	0.75	0.83
Cs	0.51	0.76	1.42	0.08	0.25	0.06	0.09	0.08	5.18
Ba	103	54	110	120	77	108	47	97	322
La	3.04	2.10	2.74	5.39	4.87	13.05	12.96	3.07	10.05
Ce	8.14	6.08	7.37	8.35	7.94	25.34	26.53	7.00	21.29
Pr	1.24	1.00	1.18	0.83	1.00	3.09	3.31	0.97	2.78
Nd	6.43	5.58	6.36	3.04	4.50	13.38	14.57	4.71	12.75
Sm	1.94	1.94	2.13	0.54	1.23	3.20	3.60	1.37	3.26
Eu	0.66	0.63	0.71	0.65	0.34	0.96	1.05	0.52	1.02
Gd	2.29	2.43	2.61	0.65	1.25	3.35	3.86	1.72	3.56
Tb	0.44	0.49	0.51	0.10	0.21	0.57	0.68	0.32	0.64
Dy	2.81	3.24	3.38	0.57	1.64	3.54	4.23	2.10	4.12

ACCEPTED MANUSCRIPT

Ho	0.56	0.65	0.69	0.12	0.33	0.71	0.85	0.42	0.83
Er	1.68	1.96	2.02	0.40	1.02	2.15	2.57	1.28	2.54
Tm	0.28	0.33	0.34	0.07	0.17	0.35	0.42	0.21	0.41
Yb	1.71	1.94	2.05	0.50	1.22	2.18	2.63	1.31	2.57
Lu	0.28	0.32	0.34	0.10	0.21	0.36	0.42	0.21	0.42
Hf	1.04	1.20	1.28	2.27	2.58	1.68	1.87	0.66	1.73
Ta	0.08	0.08	0.10	0.07	0.17	0.15	0.23	0.08	0.28
Pb	0.31	0.68	8.90	5.67	0.97	3.40	0.05	0.15	0.53
Th	0.45	0.22	0.31	0.35	0.98	2.42	2.55	0.36	1.15
U	0.16	0.06	0.12	0.11	0.18	0.52	0.58	0.09	0.30
$^{143}Nd/^{144}Nd$ (m)	0.512926	0.513029	0.512993	0.512940	-	-	0.512844	-	0.512889
2 sigma error	0.000010	0.000009	0.000009	0.000014	-	-	0.000012	-	0.000010
$^{147}Sm/^{144}Nd$	0.182505	0.210306	0.202584	0.107449	-	-	0.149461	-	0.154665
$^{143}Nd/^{144}Nd$ (i)	0.512830	0.512919	0.512887	0.512884	-	-	0.512765	-	0.512808
εNd (i)	5.76	7.49	6.87	6.81	-	-	4.50	-	5.32
$^{87}Sr/^{86}Sr$ (m)	0.707628	0.704353	0.705370	0.703991	-	-	0.704608	-	0.703927
2 sigma error	0.000015	0.000014	0.000012	0.000017	-	-	0.000038	-	0.000013
$^{87}Rb/^{86}Sr$	0.186009	0.009763	0.065767	0.008491	-	-	0.082508	-	0.021408
$^{87}Sr/^{86}Sr$ (i)	0.707015	0.704321	0.705153	0.703963	-	-	0.704336	-	0.703856

Table 1. Representative major oxides, trace elements and Sr-Nd isotopes of the Muslim Bagh ophiolite and the Bagh complex

Rock	**Gabbro**	**Gabbro**	**Bbc**	**Bbc**	**Bbc**	**Bhm**	**Bhm**	**Bhm**	**Bhm**	**Bhm**
Sample	**C47**	**C191**	**C62**	**C63**	**C123**	**C13**	**C58**	**C59**	**C61**	**C126**
SiO_2	46.39	46.08	60.03	48.24	47.79	39.25	45.13	34.12	42.88	43.65
TiO_2	0.08	0.10	1.11	0.98	0.79	3.17	2.98	2.71	3.24	3.72
Al_2O_3	29.58	20.74	14.09	15.05	13.47	12.05	9.64	9.01	11.03	13.04
Fe_2O_3	3.06	5.22	9.99	9.28	9.42	11.52	12.42	11.08	12.08	12.08
MnO	0.05	0.09	0.13	0.17	0.20	0.18	0.07	0.15	0.15	0.17
MgO	3.70	7.76	2.30	8.18	7.75	8.39	7.94	11.55	10.61	7.23
CaO	14.90	17.55	6.63	10.28	10.29	15.21	11.20	15.27	12.90	10.12
Na_2O	1.11	0.46	5.93	3.25	6.49	2.35	6.40	1.71	1.24	1.06
K_2O	0.11	0.03	0.09	0.60	0.30	0.99	0.31	1.33	1.75	5.21
P_2O_5	0.01	0.00	0.22	0.07	0.06	0.80	0.57	0.51	0.78	0.67
LOI	1.62	0.75	0.56	3.71	2.63	6.57	3.70	11.95	3.55	3.56
Total	100.62	98.78	101.22	99.92	99.27	100.83	100.68	99.70	100.57	100.92
Sc	16.1	36.1	25.9	39.2	38.9	19.9	23.0	23.1	22.5	17.9

ACCEPTED MANUSCRIPT

V	31	147	291	285	213	185	260	112	216	263
Cr	7	100	2	527	523	372	797	740	497	150
Co	10.2	26.7	18.6	43.3	46.3	53.8	58.5	54.0	56.7	55.3
Ni	41	53	85	1516	1090	1775	423	968	725	221
Cu	37.6	102.3	54.2	35.0	30.5	58.3	52.9	47.6	79.9	76.5
Zn	19.8	34.5	92.0	106.7	143.0	166.4	117.2	118.2	113.3	213.7
Ga	12.7	10.3	17.7	16.6	13.5	20.8	14.4	18.1	20.2	26.9
Rb	1.4	0.5	1.0	9.5	3.9	18.9	3.3	33.4	27.1	96.1
Sr	429	286	108	190	282	562	168	196	619	1285
Y	1.1	1.5	28.2	26.0	20.9	27.9	24.0	23.0	29.4	33.3
Zr	8	8	83	54	49	225	192	197	287	255
Nb	0.36	0.50	2.37	4.09	0.57	29.54	23.65	23.34	26.97	42.94
Sn	1.71	1.64	1.21	7.25	0.84	1.66	2.43	2.22	3.04	1.75
Cs	0.06	0.10	0.27	0.43	0.25	1.45	0.50	2.65	0.76	2.35
Ba	75	28	49	123	125	415	775	176	1570	1521
La	0.28	0.05	11.21	2.81	1.67	61.79	39.38	45.60	69.72	65.76
Ce	0.75	0.18	21.98	6.92	4.78	117.28	79.10	92.10	131.07	118.96
Pr	0.10	0.04	3.04	1.24	0.91	13.99	9.96	10.87	15.57	13.89
Nd	0.51	0.35	13.37	6.36	4.97	52.27	39.67	42.18	57.82	51.51
Sm	0.17	0.16	3.36	2.27	1.77	9.62	9.89	9.90	13.92	12.58
Eu	0.12	0.10	1.13	0.76	0.74	3.04	2.70	2.46	3.57	3.13
Gd	0.24	0.32	3.60	2.59	2.23	8.37	7.01	6.93	9.22	8.49
Tb	0.04	0.06	0.63	0.47	0.44	1.13	0.98	0.94	1.20	1.13
Dy	0.27	0.36	4.74	3.92	3.44	6.00	5.29	5.05	6.31	6.05
Ho	0.05	0.07	0.98	0.81	0.74	1.00	0.88	0.83	1.06	1.04
Er	0.14	0.19	2.65	2.38	2.01	2.38	2.06	2.00	2.55	2.62
Tm	0.02	0.03	0.45	0.37	0.33	0.31	0.26	0.26	0.32	0.34
Yb	0.14	0.17	2.98	2.49	2.15	1.91	1.62	1.54	1.96	2.15
Lu	0.02	0.03	0.48	0.41	0.35	0.29	0.23	0.23	0.29	0.29
Hf	0.17	0.16	2.23	1.46	1.31	5.85	4.66	4.70	6.82	6.53
Ta	0.02	0.03	0.12	0.24	0.03	2.09	2.05	2.25	2.18	3.64
Pb	0.59	3.72	5.03	7.37	4.32	6.29	5.74	5.32	8.97	12.39
Th	0.10	0.11	1.66	0.39	0.31	6.86	4.17	4.91	6.67	7.94
U	0.03	0.01	0.40	0.08	0.05	1.62	1.07	1.73	1.98	2.27
^{143}Nd/^{144}Nd (m)	-	0.512848	-	-	0.512950	-	0.512797	-	-	-
2 sigma error	-	0.000022	-	-	0.000011	-	0.000010	-	-	-
^{147}Sm/^{144}Nd	-	0.276526	-	-	0.215427	-	0.120309	-	-	-
^{143}Nd/^{144}Nd (i)	-	0.512703	-	-	0.512752	-	0.512733	-	-	-
εNd (i)	-	3.27	-	-	5.75	-	3.89	-	-	-

ACCEPTED MANUSCRIPT

$^{87}Sr/^{86}Sr$ (m)	-	0.704313	-	-	0.706821	-	0.705397	-	-	-
2 sigma error	-	0.000012	-	-	0.000014	-	0.000017	-	-	-
$^{87}Rb/^{86}Sr$	-	0.001750	-	-	0.013840	-	0.019631	-	-	-
$^{87}Sr/^{86}Sr$ (i)	-	0.704307	-	-	0.706741	-	0.705332	-	-	-

Abreviations

Mds - mafic dyke swarm; Sd - sheeted dykes; Plag Gr - Plagiogranite;

Bbc - basalt from basalt-chert unit; Bhm - basalt from hyaloclastite-mudstone unit

ACCEPTED MANUSCRIPT

ACCEPTED MANUSCRIPT

Graphical abstract

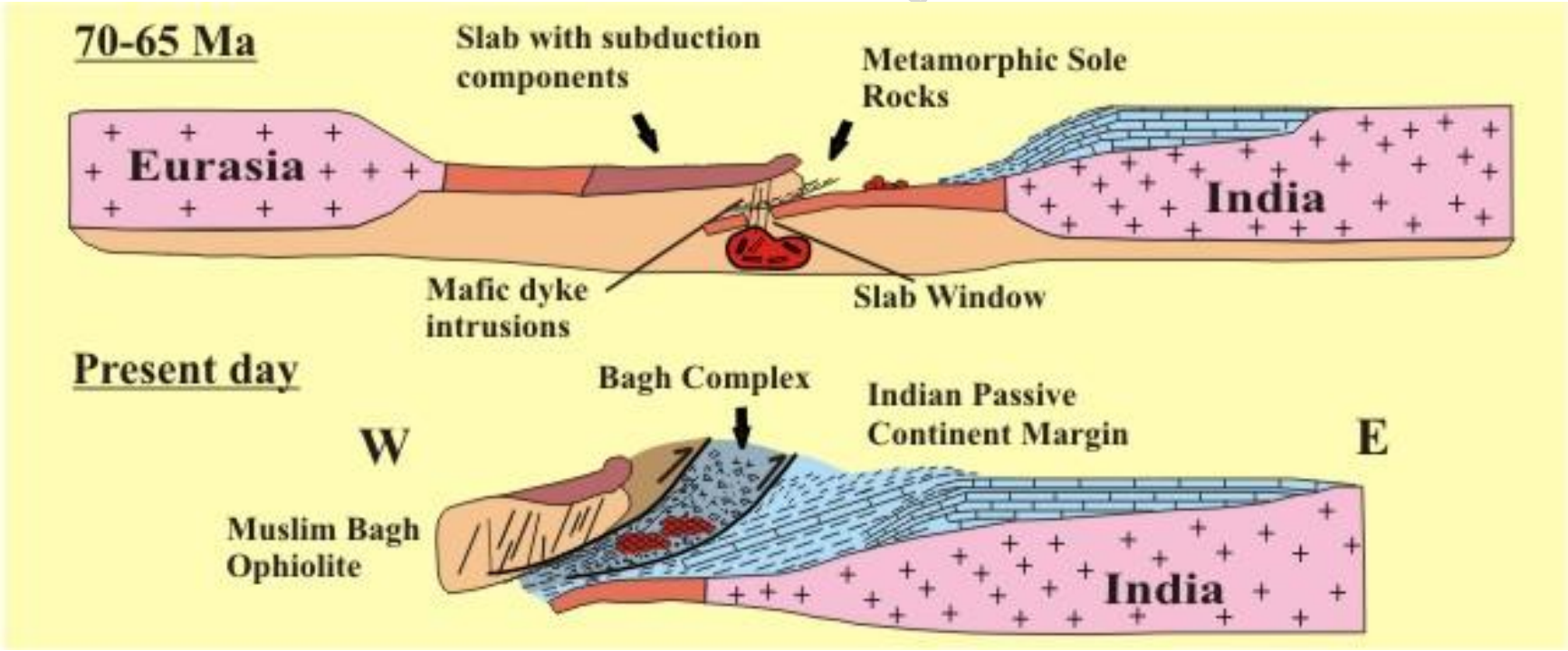

ACCEPTED MANUSCRIPT

Highlights

7. The Muslim Bagh Ophiolite formed in a supra-subduction zone tectonic setting.

8. The source region of the sheeted dykes is MORB-like with a subduction input.

9. The Bagh Complex basalts are contaminated with continental crust

ACCEPTED MANUSCRIPT